

Interactive comment on “An overview of the lightning and atmospheric electricity observations collected in Southern France during the HYdrological cycle in Mediterranean EXperiment (HyMeX), Special Observation Period 1” by E. Defer et al.

Dr Poelman (Referee)

dpoelman@oma.be

Received and published: 12 August 2014

We would like to thank Dr Poelman for his constructive review. All comments have been addressed as detailed in the following document and in the revised version of the paper.

This manuscript describes the observations performed within the PEACH experiment in the framework of the HyMeX campaign, and specifically during SOP1. The different instruments used during SOP1, as well as the operational Lightning Location Systems and some results of specific observations are addressed.

The manuscript fits well within the scope of Atmos. Meas. Tech. and could be a valuable contribution to the literature. However, there are some issues that should be addressed:

Main comments:

- There is an excessive use of brackets “(…)” in the text, which makes it sometimes hard to read. To improve the readability of the manuscript, most of the text within the brackets should be incorporated within the text.

Response : The brackets were originally used to concise the content of the paper. Now most brackets have been removed and the text adapted.

- Abstract: p8015 L18-L26 “A description of the different instruments ... are discussed.” This text belongs to the Introduction section. The ‘Abstract’ should contain the results/outcome of the paper, and not just a description of the different Sections.

Response : We have replaced the following part of the abstract “A description of the different instruments deployed during the field campaign as well as the available datasets is given first. Examples of concurrent observations from radio frequency to acoustic for regular and atypical lightning flashes are then presented showing a~rather comprehensive description of lightning flashes available from the SOP1 records. Then examples of storms recorded during HyMeX SOP1 over Southeastern France are briefly described to highlight the unique and rich dataset collected. Finally, future steps required for the delivery of reliable lightning-derived products to the HyMeX community are discussed” by “Herein we present an overview of the PEACH project and its different instruments. Examples are discussed to illustrate the comprehensive and unique lightning dataset, from radio-frequency to acoustics, collected during the SOP1 for lightning phenomenology understanding, instrumentation validation, storm characterization and modeling.”

- 1 Introduction: p8019 L14-L19: I am missing the goal of this paper. The authors could provide a small paragraph at the end of the introduction containing what the authors want to bring to the

scientific community with this paper, why has it been written? This is partly described in Sect. 2, but a short description is at place at the end of the introduction.

Response : One small paragraph has been added at the end of the introduction section, just prior the brief description of the content of the paper as follows:

“Lightning detection is definitively useful to monitor thunderstorms and to help improve severe weather simulations. Among the open scientific questions related to the electrical activity, are the links between microphysics, kinematics and lightning activity, the use of the lightning information in multi-sensor rainfall estimation and the lightning-flash phenomenology. In the following we describe the rationale for dedicated lightning observations to characterize the electrical properties of Northwestern Mediterranean storms during a dedicated campaign of the HYdrological cycle in the Mediterranean EXperiment (HyMeX) program (Ducrocq et al., 2013). First, the HyMeX project is briefly described in Sect. 2. The scientific questions and the observational strategy of the HyMeX lightning task team, including instruments and models, are described in Sect. 3. Section 4 presents an overview of the observations collected at flash, storm and regional scales. Section 5 then discusses the perspectives by listing out the next steps of the data analysis as well as the data and products made available to the HyMeX Community.”

- 2 The HyMeX program: p8020 L8: “Super sites”. Explain a bit more what these sites are. How were these chosen? What makes them different from other sites? This is somewhat indicated in Sect. 3 L24 but could be described earlier.

Response : A super site over land or the ocean gathers research instruments dedicated to the study of specific processes. We propose the following to detail a bit more the notion of super site.

“Those equipments were deployed at or near super sites where dedicated research instruments are gathered to document specific atmospheric processes c.”

- 3 The PEACH experiment: p8020 L20. Maybe one can start first with the goals of PEACH. For instance, part of Sect. 3.1. could be placed here to describe the scientific objectives.

Response : We would prefer to keep the current structure of the paper as the two first paragraphs describe briefly the nature of the electrical activity in the Mediterranean Basin and the relevance of the lightning detection for storm monitoring over the Mediterranean Sea. Then we list the scientific objectives of the PEACH project and its observational/modeling strategy.

- p8023: LMA, EFM, SLA are all described in a designated subsection. However, this is not the case for INR. Therefore, the authors could consider to include a subsection explaining the main parameters of the INRs, as has been done for the other instruments.

Response : The induction rings (INR) were built just before the field deployment and were not enough tested before their deployment and operation during the field campaign. They all failed due to non-reliable electronic chips. It is why we did not originally describe them in the paper. Notice that the INR measurements were aimed to provide some ground-truth on the actual electrical charges carried by the raindrops at the ground for a comparison and verification of simulated charge distribution at ground level provided by the cloud-resolving model MESO-NH. As suggested by the Reviewer we now include one section describing the principle of an induction ring as well as the explanation of the failure. Here is the text that has been inserted:

” The electric charge carried by raindrops can easily be detected and measured by a simple apparatus commonly called induction ring. This sensor is constituted of a

cylindrical electrode (the ring) on the inner surface of which induced electric charges appear by electrostatic influence when a charge raindrop enters the sensor. When the drop leaves the sensor, the induced charges disappear. The cylindrical electrode is connected to an electrometer and the current signal induced by the passing of a charged drop (a bipolar current impulse) is sampled at a rate of 2000 Hz. It is amplified and integrated by an electronic circuitry that directly provides the charge signal. This one appears as a single pulse with amplitude and length proportional to the charge and to the velocity of the drop, respectively. The actual charge is deduced from the calibration of the sensor. If the drop collides with the induction cylinder, the pulse signal exhibits a slow exponential decay (MacGorman and Rust, 1998) that is easily recognizable in the post data processing. In this case, the raindrop charge that is fully transferred to the induction cylinder is determined by a specific calibration. The charge measurement sensitivity ranges from about  $\pm 2$  pC to  $\pm 400$  pC. Furthermore, the charge signal duration at mid height can be used to determine the size of the charged raindrops provided the relationship between size and fall velocity in function of the actual temperature and pressure (Beard, 1976).

Such measurement provides key information on the electric charge carried by the rain at the ground to validate numerical modeling. It documents the spectrum of charged drops and helps deduce the proportion of charged drops within the whole drop population by comparing its spectrum with the one measured by a disdrometer. Four induction rings were built and operated during the SOP1, mainly along the South to North axis at the foothills of the Massif Central where most of high precipitating events occur. Unfortunately, only few events passed above the sensors and in these rare cases, the main electronic component of the induction rings suffered dysfunction that were not detected during the laboratory tests, so no valuable INR data are available for the SOP1.”

- 3.3 Operational Lightning Location Systems: The writing style of the subsections concerning the description of the OLLS is not coherent. The authors could slightly rewrite these sections in order to converge the writing style of the OLLS subsections.

Response : As suggested by the Reviewer, the subsections dealing with the description of the OLLSs have been rewritten with similar information. See the different sections describing the OLLSs.

- Concerning the description of all the OLLS: It would be worth to include some LA and DE values + references, if possible within the region/neighborhood of HyMeX SOP1.

Response : Some numbers are now given in the different subsections describing the OLLSs. We would like to stress out that one of the objectives of the investigations performed with the HyMeX SOP1 data is to assess in the SOP1 region both DE and LA for all operational networks.

- 3.5 Modeling: This section is out of the scope of this paper and no further results are presented in this paper on the modeling aspects. Maybe the authors could just make a comment concerning the modeling efforts in stead of including sect. 3.5.1 and 3.5.2 in the manuscript. For instance p8034 L22-L26 can be removed to Section 5 Prospects.

Response : The Authors was discussed on that question before the submission. Our strategy is to use as much instruments as possible, and models are instruments for us, to tackle the different scientific questions investigated here. So we would like to keep the Modeling section as it is now. Some modeling exercises have already been performed, but are not discussed here. s

- 4.1 SOP1 Climatology: The authors should include a bit more info on the climatology during SOP1: How many thunderstorm days were observed in the region of interest (describe Fig. 2), how many flashes have been observed during SOP1?, ...

Response : We have provided some additional information on the lightning climatology. Figure 2 has now one extra panel showing the number of lightning days on the yearly basis for the SOP1 duration. No reference on actual number of flashes is given due to the successive upgrade of Météorage network.

Note that we performed a set of investigations on the lightning climatology based on Météorage data that were used for the definition of the HyMeX SOP1 Implementation Plan.

We propose the following text now:

“The year 2012 was rather weak in terms of lightning activity over the center of the SOP1 domain. The electrical activity was mainly located in the far Northern part of Cévennes-Vivarais, and was more pronounced along the Riviera coastline and over the Ligurian Sea (Fig. 2b). About 0.3% of the 5 km x 5 km pixels of the year 2012 contribute to more than 20% of the 16-year climatology. Over the 500-km side domain plotted in Fig.2a and 2b, and for a period ranging from 5 September to 6 November, the total number of days with lightning activity in 2012 reached a value of 44 days, slightly below the average value for the 16 years of interest (Fig. 2c).”

Minor comments and proposed editorial changes:

Affiliations: Nowcast (with capital letter) and Météo-France (include hyphen)

Response : nowcast has been replaced by Nowcast GmbH, Météo France by Météo-France.

Abstract:

- P8015 L1: The PEACH project (Projet ...) is the ...

Response : Modified.

- P8015 L7: During the HyMeX SOP1 (Special Observation Period) from 5 September to 6 November 2012, four ...

Response : Modified.

- P8015 L8: (OLLs) under which ATDNET, EUCLID, LINET, ZEUS, and the ... + I think it is 'ATDnet' and not 'ATDNET'

Response : Modified.

- P8015 L23: Then, examples ...

Response : Corrected.

- p8015 L24: Finally, future steps required for the delivery ...

Response : Modified as suggested.

1 Introduction:

- P8016 L10: ... ice particles, temperature and liquid water content.

Response : Corrected.

- P8016 L16: However, such an electric field intensity is one order ...

Response : Corrected.

- P8016 L19: or hydrometeor interactions present in high electric fields ...

Response : Corrected as suggested.

- P8016 L22: exceeds a threshold: threshold is of the order of? Give an idea of this.

Response : of a few kV/m. Added in the text.

- P8016 L23: Hence, it is clear that the lightning activity of a thundercloud ...

Response : Corrected as suggested.

- P8016 L26: occur in clouds, while ...

Response : Corrected as suggested.

- P8016 L27: (positive) charge to the ground.

Response : Corrected as suggested.

- P8016 L28: electromagnetic radiation when connecting to the ground.

Response : Corrected as suggested.

- P8017 L2: connections to the ground (references?)

Response : We proposed among others the following references:

Mäkelä, A., T. J. Tuomi, and J. Haapalainen (2010), A decade of high-latitude lightning location: Effects of the evolving location network in Finland, *J. Geophys. Res.*, 115, D21124, doi:10.1029/2009JD012183.

Orville, R. E., G. R. Huffines, W. R. Burrows, and K. L. Cummins, (2011), The North American Lightning Detection Network (NALDN)—Analysis of Flash Data: 2001–09. *Mon. Wea. Rev.*, 139, 1305–1322.

- P8017 L8: rephrase: 'A lightning flash then consists in a multi-scale physical process'

Response : We propose "A lightning flash is then constituted of a series of multi-scale physical processes".

- P8017 L9: ... over large distances of a few km or more.

Response : Corrected as suggested.

- P8017 L11: ... have been developed to detect and locate these ...  
Response : Corrected as suggested.

- P8017 L13: For instance, ...  
Response : Corrected as suggested.

- P8017 L14: ... borne sensors detect electromagnetic ...  
Response : Corrected as suggested.

- P8017 L21: rephrase: 'to provide the most comprehensive description for analyzing in details the lightning flashes', e.g.: provide the most comprehensive description in order to analyze in great detail ...  
Response : Corrected as suggested.

- P8017 L29: Flash rates ...  
Response : Corrected as suggested.

- P8018 L2: Flash rates reach a peak value ...  
Response : Corrected as suggested.

- P8018 L9: "(IC+CG)" already defined on p8017 L27 => can be removed  
Response : Removed.

- P8018 L9: total lightning activity is a more ...  
Response : Corrected.

- P8018 L22: For instance, ...  
Response : Corrected.

- P8018 L24: ... in the pioneering model ...  
Response : Corrected.

- P8018 L25: Altaratz et al. (2005). Based on the references, it should be (2005), not (2003)  
Response : Corrected.

- P8019 L4: CRMs are the preferred modeling tools ...  
Response : Corrected.

- P8019 L8: ... and by Saunders et al. (1991). Those disagree ... (make a new sentence, original sentence is too long)

Response : We propose “A key challenge in simulating cloud electrification mechanisms is the lack of agreement in the community about the relevance of each of the non-inductive charging diagrams published by Takahashi (1978) and by Saunders et al. (1991). Those diagrams disagree in some way because the protocol of the laboratory experiments was different.”

- P8019 L15: ... strategy of the HyMeX ...

Response : Added.

- P8019 L17: Section 5 then discusses the perspectives ...

Response : Corrected.

2 The HyMeX program:

- P8019 L23: ... and lead to expensive property damage.

Response : Corrected.

- P8019 L24/L25: remove ‘dedicated to the hydrological cycle in Mediterranean’ since this is exactly what HyMeX stands for.

Response : Removed as suggested.

- P8019 L26: As part of this ...

Response : Corrected as suggested.

- P8019 L27: ... during 2 months from 5 September 2012 to 6 November 2012 over the Northwestern ...

Response : Modified as suggested.

- P8020 L7: ... lidar, and rain gauges

Response : Added as suggested.

- P8020 L10: Additionally, various

Response : Added as suggested.

- P8020 L13 & L15: two times ‘autumn’, the last one on L15 could therefore be removed

Response : Removed as suggested.

3 The PEACH experiment:

- P8021 L5: ... geostationary satellites can offer ...

Response : Corrected.

- P8021 L15: However, further ...

Response : Added as suggested.

- P8021 L17: ... of the parent clouds ...

Response : Corrected.

- P8021 L15-L20: Last sentences could be split into 2 sentences to improve readability.

Response : We propose now “However, further scientific investigations are required to document the links between the lightning activity and the dynamical and microphysical properties of the parent clouds in continental and maritime Mediterranean storms. In addition it is necessary to identify the key parameters derived from OLLS records alone or in combination with other meteorological observations to provide suitable proxies for a better storm tracking and monitoring over the entire Mediterranean Basin.”

3.1 Scientific objectives and observational/modeling strategy:

- P8021 L21: The scientific objectives, i.e. p8021 L22 – p8022 L18, could be removed and replaced at the beginning of Sect. 3. Therefore, the title could become ‘3.1 observational and modeling strategy’. Thus, p8022 L19 could be the new start of Sect.

Response : As mentioned earlier we would prefer to keep the current structure of the paper.

3.1.

- P8021 L25: Who are member of the PEACH team, this hasn't been described yet.

Response : We propose “The PEACH team, composed of the Authors of the present article, identified five observational- and modeling-based scientific objectives in relation to HyMeX goals:”

- P8021 L26: and modeling-based scientific ... in relation to the HyMeX goals: ..

Response : Corrected.

- P8022 L10: ... to HPEs and flash-floods ...

Response : Corrected.

- P8022 L12: observations to improve monitoring

Response : Replaced.

- P8022 L13/L14: try not to use “(…)”

Response : The parentheses are removed.

- P8023 L3: (SLAs), as well as

Response : Added.

- P8023 L6: Finally, ...  
Response : Added.

- P8023 L9: (MBA and MPA, respectively)  
Response : Added.

- P8023 L11: also includes a range of numerical ... + rephrase 'hosting or not a lightning/ electrification scheme'  
Response : We propose "The PEACH project also includes two cloud resolving models, MesoNH with its electrification and lightning scheme, and WRF."

- P8023 L21: remove ', of course,'  
Response : Removed.

- P8023 L23: In addition, ...  
Response : Added.

- P8023 L25: ... help to investigate ...  
Response : Corrected.

- P8023 L28: of the lightning flashes, as well as ...  
Response : Added.

- P8023 L29: ... tHunderclouds, allows ...  
Response : Corrected.

- General comment: 'in situ' or 'in-situ': be consistent throughout the paper  
Response : 'in situ' is used throughout the paper now.

- P8024 L2: Finally, ...  
Response : Added.

- P8024 L7: As a result, ...  
Response : Added.

- P8024 L9/L10: three times 'stage' in 1 sentence is a bit too much. Make use of synonyms.  
Response : Sorry for the phrasing. We propose "As a result, the HyMeX SOP1 experiment is probably the first ambitious field experiment in Europe to offer such comprehensive description of lightning activity and of its parent clouds over a mountainous area from the early stage to the

decaying phase of the sampled electrical storms.”

- P8024 L11: ... in conjunction with the operational network of Météo-France ...

Response : Modified as suggested.

- P8024 L13: start a new paragraph with: ‘In the following we ...’. However, this sentence is too long and could be split into 2 sentences: In the following we give some ... observations. Several other studies are underway to investigate the ...and rain patterns, as derived ... + However: ‘in the following’ is not true in this case: ‘in the following’ the instruments are described in Sect. 3.2, so text should be changed accordingly.

Response : We propose “In this article we give some examples of only atmospheric electricity observations. Several studies are underway on the electrical properties of thunderstorms relatively to cloud properties like cloud structure, microphysics and rain patterns as derived from radar and satellite observations and in situ measurements.”

3.2.1 The HyMeX Lightning Mapping Array (HyLMA):

- P8025 L10: what are the errors at 300km?

Response : We used the same program as the one used in Thomas et al. (2004) but with the locations of the 12 HyLMA stations and we obtained a theoretical error of location < 1 km at 200 km range.

3.2.3:MBA/MPS

- P8026 L3: (MBA) and a microphone array (MPA).

Response : Added.

- P8026 L10: ... has a sensitivity of a few ...

Response : Corrected.

- P8026 L24: The data from each sensor of the arrays were ...

Response : Modified as suggested.

3.2.4: EFM

- P8027 L8: include space between ‘etc. The’

Response : Inserted.

- P8027 L9: ... due to the variety ...

Response : Corrected.

- P8027 L11: ... irregularities, and the charge ...

Response : Added.

- P8027 L17/L19: orientated -> oriented

Response : Corrected.

- P8027 L15/L20: field mills / field-mills: be consistent

Response : 'field mill(s)' is used throughout the paper now.

- P8027 L25: avoid "(...)"

Response : We propose "The polarity of the field is positive when the field points upward and the electric field is created by negative charge overhead."

### 3.2.5: VFRS

- P8028 L2: VRFS acronym has been already introduced earlier in the text, so no need to do this again.

Response : OK. It is removed now. We propose "The VFRS instrument".

- P8028 L23: scenario, e.g. location . . .of the storms, the VRFS . . .

Response : Parentheses removed.

### 3.2.6: Locations and status of the research instruments

- P8029 L12: Finally, ...

Response : Added.

- P8029 L21: distributed to the HyMeX Community.

Response : Added.

- P8029 L22: Additionally, ATDnet ...

Response : Added.

- P8029 L23: to the HyMeX ...

Response : Added.

### 3.3.2: EUCLID/Meteorage

- P8031 L9: As of August 2009: what is the present status during SOP1 of EUCLID/Météorage?

### 3.3.3: LINET

- P8032 L7: remove "(total lightning)", since it looks now as if cloud strokes = TL

- P8032 L8: Typical baselines

- P8032 L12: is somewhat lower: any idea how much lower?

### 3.3.4 ZEUS

- P8032 L19 : remove 'Very Low Frequency', since the VLF acronym has been introduced already earlier in the manuscript

- P8032 L22/L23: remove '( ... )'

- P8032 L25/L26: use other word for 'major'

Response : New sections describing the OLLSs were introduced in the paper, with corrections as suggested by the Reviewer. The section is now as follows:

### ***“3.3 Operational Lightning Locating Systems***

#### **3.3.1 ATDnet**

The UK Met Office VLF ATDnet (Arrival Time Differencing NETWORK) lightning location network takes advantage of the long propagation paths of the VLF (frequency range) sferics emitted by lightning discharges, which propagate over the horizon via interactions with the ionosphere (Gaffard et al., 2008). The ATDnet network consists of 11 that regularly contribute to the “operational network”, plus sensors distributed further afield. The waveforms of VLF sferics received at the ATDnet sensors are transmitted to a central processor in Exeter, where the waveforms are compared in order to estimate arrival time differences. These arrival time differences are compared with theoretical arrival time differences for different locations, in order to estimate the most likely source location. Current ATDnet processing requires four ATDnet sensors to detect a lightning stroke in order to be able to calculate a single, unambiguous source location. ATDnet predominantly detects sferics created by CG strokes, as the energy and polarization of Sferics created by CG return strokes can travel more efficiently in the Earth–Ionosphere waveguide, and so are more likely to be detected at longer ranges than typical IC discharges. ATDnet location uncertainties within the region enclosed by the network of sensors are on the order of a few kilometers, i.e. suitable for identifying electrically active cells.

#### **3.3.2 EUCLID**

The EUCLID network (EUropean Cooperation for LIghtning Detection) is a cooperation of several European lightning detection networks (Austria, Finland, France, Germany, Italy, Norway, Portugal, Slovenia, Spain, and Sweden) that operate state-of-the-art lightning sensors. As of August 2009 the EUCLID network employs 137 sensors, 5 LPATS III, 18 LPATS IV, 15 IMPACT, 54 IMPACT ES/ESP, 3 SAFIR and 42 LS7000 sensors (oldest to newest), all operating over the same frequency range (1 kHz -350 kHz) with individually-calibrated gains and sensitivities. Data from all of these sensors are processed in real-time using a single common central processor, which also produces daily performance analyses for each of the sensors. This assures that the resulting data are as consistent as possible throughout Europe. In fact, the Europe-wide data produced by EUCLID is frequently of higher quality than the data produced by individual country networks, due to the implicit redundancy produced by shared sensor information. Since the beginning of the cooperation the performance of the EUCLID network has been steadily improved, e.g. with improved location algorithms, with newer sensor technology and by adapting sensor positions because of bad sites. The flash/stroke detection efficiency (DE) of the EUCLID network in the south of France was determined to be 90%/87% for negative and 87%/84% for positive discharges but for a time period where a close sensor was out of order (Schulz et al., 2014). Therefore the values should be rated as lower limits of EUCLID DE in this region. The location accuracy was determined to be 256 m but based on 14 strokes only.

#### **3.3.3 LINET**

The LINET system is a modern lightning detection network in the VLF/LF domain (5 kHz – 100 kHz) developed by nowcast GmbH (Betz et al., 2008, 2009). LINET Europe consists of more than 120 sensors placed in 25 countries. Each of them includes a field antenna, a GPS antenna and a field processor. The field antenna measures the magnetic flux produced by a lightning. The processor evaluates this signal and combines it with the

accurate time provided by the GPS antenna. Compact data files are then sent to a central processing unit where the final stroke solutions are generated. Accurate location of strokes requires that the emitted signal is detected by many sensors. Reported strokes are based on reports from at least 5 sensors. Strokes are located using the Time-Of-Arrival (TOA) method. LINET detects also cloud strokes, and can distinguish between CG strokes and IC strokes. Typical baseline of LINET systems are 200 km between adjacent sensors, allowing very good detection efficiency, even for very weak strokes (< 10 kA), whereby an average statistical location accuracy of ~200 m is achieved. However, in the HyMeX area in Southern France the baselines are longer and, thus, the efficiency is somewhat lower than in most other LINET network areas.

### 3.3.4 ZEUS

The ZEUS network is a long-range lightning detection system, operated by the National Observatory of Athens. ZEUS system comprises six receivers deployed in Birmingham (UK), Roskilde (Denmark), Iasi (Romania), Larnaka (Cyprus), Athens (Greece), Lisbon (Portugal), the latter being relocated to Mazagon (Spain). ZEUS detects the impulsive radio noise emitted by a lightning strike in the Very Low Frequency (VLF) spectrum between 7 and 15 kHz. At each receiver site an identification algorithm is executed that detects a probable sferics candidate, excludes weak signal and noise and is capable of capturing up to 70 sferics per second. Then the lightning location is retrieved (at the central station) using the arrival time difference technique. Further details on ZEUS network are given in Kotroni and Lagouvardos (2008). Lagouvardos et al. (2009) have compared ZEUS system with the LINET system over a major area of Central-Western Europe where the latter system presents its major efficiency and accuracy and found that the location error of ZEUS was 6.8 km and the detection efficiency 25%. These numbers are applicable also for the SOP1 domain. The authors found also that while ZEUS detects cloud-to-ground lightning it is also capable to detect strong IC lightning. At this point it should be stated that the statistical analysis showed that ZEUS is able, with high accuracy, to detect the occurrence of lightning activity although it underdetects the actual number of strokes.”

#### 3.4: Instrumentation during EOP and LOP

- General comment: Maybe this section can be moved to Sect. 5 ‘Prospects’ section, since this paper deals only with SOP1 observations

Response : This section was placed here in order to show that the PEACH team is providing an expertise on lightning activity, mainly with the operational networks, for HyMeX EOP and LOP activities as others supersites are still running and future local field campaigns over the Mediterranean Basin are expected. So we would like to keep that section in its current place in the paper.

- P8033 L3: For instance, ...

Response : Added.

- P8033 L4: ... web site, while ...

Response : Added.

- P8033 L5: are delivered to the HyMeX database.

Response : Corrected.

- P8033 L6: '12 LMA': however, on p8029 L16: '11 stations' => make consistent

Response : This is a new LMA network that has been installed in Corsica and has been operated since mid-July 2014. It is not the same network as the one operated during SOP1, which was borrowed to NASA Marshall Space Flight Center group.

From the Reviewer comment, we have added the following precision in the former p8029 L16 "The 12<sup>th</sup> HyLMA station was online early beginning of September 2012".

#### 4.1 SOP1 climatology

- P8036 L7: Interestingly, this new ...

Response : Added.

#### A regular IC

- P8036 L12: an example of a regular

Response : Added.

- P8036 L13: What is meant with #06?

Response : It is the number of the IOP event. We rephrase it as follows "Figure 3 shows an example of a regular IC flash recorded by HyLMA during SOP1 Intensive Observation Period (IOP) IOP-06 on 24 September 2012".

- P8036 L16: Do not use '( and ')', just make it into a normal sentence. For instance: 'For more information on ... the interested reader is referred to Thomas ...'

Response : We propose the following "It was composed of 2510 VHF sources as reconstructed from at least 7 HyLMA stations and  $\chi^2 < 1$ . For more information on the definition of the parameters associated to each LMA source the interested reader is referred to Thomas et al. (2004). The VHF sources were vertically distributed between 4 and 12 km height (Fig. 3d)."

- P8036 L17: rephrase: 'and distributed between 4 and 12 km height.'

Response : See previous response.

- P8036 L19: msl? => asl?

Response : "asl". Corrected.

- P8036 L23: propagated faster: as evidenced from?

Response : As evidenced from the actual distances traveled by the negative leaders compared to the ones traveled by the positive leaders during the same temporal gap. We inserted the previous phrase in the paper now.

- P8037 L2: Finally, ...

Response : Corrected.

A regular negative CG

- P8037 L7: ... and the different OLLS, but ...

Response : Corrected.

- P8037 L8: at close range of about 25 km by the VRFS instruments. VRFS has been already explained, so 'FM and video camera' can be removed.

Response : Modified as suggested.

- P8037 L11: ... 1464 VHF sources derived from at least ...

Response : Added as suggested.

- P8037 L17: rewrite a bit: ATDnet reported 7 events, whereas EUCLID identified 5 strokes ..., and LINET categorized 8 strokes as ...

Response : Modified as suggested as follows "ATDnet reported 7 events, whereas EUCLID identified 5 strokes as negative ground connections, and LINET categorized 8 strokes as negative ground connections and 1 stroke as positive ground connection"

- P8037 L23: ... close to each other ...

Response : Corrected.

- P8037 L28: remove '(...)' in the text, the same for p8038 L4

Response : Removed. And removed.

- P8038 L6: FM should become EFM as defined first on p8023 L3, also on p8038 L12/L19

Response : FM stands for the Field Measurement of VRFS. To be more precise we replace FM by Field Record at both locations pointed out by the Reviewer and in different phrases in the manuscript.

- P8038 L12: Additionally, the noisy EFM ...

Response : Added.

- P8038 L28: For instance, ...

Response : Added.

- P8039 L1: for a specific type of flash, ...

Response : Corrected.

- P8039 L2: time in UTC?

Response : Yes. It is now indicated.

- P8039 L3: the upper discharge splits in two parts, one progressing continuously upward ...  
Response : Modified as suggested.

- P8039 L5: first at a constant altitude of 8 km during 50 ms before descending and ...  
Response : Modified as suggested.

- P8039 L6: shows clearly several branches  
Response : Modified as suggested.

- P8039 L10: Additionally, ... IC events a few ...  
Response : Corrected as suggested.

- P8039 L13: This example demonstrates ...  
Response : Corrected as suggested.

- P8039 L21: The HyMeX SOP1 data offers a unique opportunity to study ...  
Response : Corrected as suggested.

- P8039 L23: ... enough and well pronounced to be detected ...  
Response : Corrected as suggested.

- P8040 L5/L6: rephrase sentence: 'HyLMA suggests that ... extensive lightning flash'  
Response : A verb was missing in the original sentence. We propose "The temporal and spatial evolution of the successive discharges mapped by HyLMA reveals that the continuous VHF signal emanated from a single but extensive lightning flash".

- P8040 L18/L19: remove '(...)'  
Response : Done.

- P8040 L21 strokes/fixes into flashes  
Response : Corrected.

- P8040 L21: This unusual flash example demonstrates ...  
Response : Modified as suggested.

- P8040 L23: Additionally, ...  
Response : Added.

- P8040 L24: Rephrase 'while others emanate from a single OLLSs'? What is meant here?

Detected by only 1 OLLS?

Response : We meant that some of the events detected by one OLLS are also detected by one, two and three other OLLSs, while sometimes some events are only reported by one single OLLS only. We rephrase as follows “Additionally, some of the events detected by one OLLS are also detected by one or more other OLLSs, while sometimes some events are reported by one single OLLS only.”

Concurrent VHF and acoustic measurements:

- P8041 L7: (with one composed of a few ...)

Response : Added.

- P8041 L9: one composed of a few

Response : Added.

- P8041 L11: one composed of a few ...

Response : Added.

- P8041 L12: Point forgotten at end of sentence: ... in the domain of interest.

Response : Added.

4.2.2 Storm and regional levels:

- Rephrase title

Response : We propose “**Examples of SOP1 daily lightning activity as recorded by HyLMA**”.

- P8042 L5: Here we discuss some storms recorded ...

Response : Modified as suggested.

- P8042 L27: in 24 h, and reached locally levels of up to 30-40 mm in Ardeche.

Response : Modified as suggested.

- P8043 L8: in the evening of 23 September ...

Response : Modified as suggested.

- P8043 L26: ... system progressing eastwards ...

Response : Modified as suggested.

- P8044 L3: include explanation for ‘while the CG flashes in the afternoon were mostly negative’?

Response : This is currently under investigation.

- P8044 L19: Additionally, ...  
Response : Added.

- P8044 L21: (French Riviera), which offers ...  
Response : Corrected as suggested.

- P8044 L23: Finally, Fig. 9F ...  
Response : Corrected as suggested.

- P8044 L27: in the complex located at ...  
Response : Added.

- P8045 L5: ... from the same flashes ...  
Response : Added.

5 Prospects:

- P8045 L12: This task will help to refine ... (or will help refining ...)  
Response : Corrected according to the 1<sup>st</sup> suggestion.

- P8045 L24: Southeastern France and which will be used in ...  
Response : Corrected as suggested.

- P8046 L4/5: remove ('...')  
Response : Removed as suggested.

- P8046 L6: should then help to identify  
Response : Corrected as suggested.

- P8046 L10: performed in the near future to ...  
Response : Corrected as suggested.

- P8046 L13: ... May 2014 for a minimum of five years.  
Response : Corrected as suggested.

- P8046 L14: ... fall where electrical activity ...  
Response : Corrected as suggested.

- P8046 L16: Finally, ...

Response : Added.

Table 1: 'Météo-France' and 'MBA/MPA'

Response : Corrected.

Fig. 1:

- In the figure M1 and M1&M2 are not indicated correctly

Response : A revised version of the figure has been provided with M1 and M1&M2 correctly indicated (see the attached figure as well as the new version of the paper provided in pdf format). See also the new figure caption "Figure 1 - Locations of PEACH instrumental sites (see Table 1 for details on site locations). M1 markers indicate VFRS locations while M2 markers indicate the few locations where additionally a second video camera was operated at the same site; sites where VFRS recorded actual lightning flashes are labeled with an extra letter 'r'. The Cévennes-Vivrais domain is also delimited by the white polygon."

- The white star in the box which is indicated now as MBA, should this become MBA/MPA?

Response : Yes. It has been modified.

Fig. 2:

- Indicate a) and b) in the figures

Response : Labels were already indicated in the lower-left corners of each panel. The labels have been moved to the upper-left corners with a white background.

- In the text 'a)' should be replaced: '... climatology a) in terms of days with ...'

- '... as sensed by' => 'based on'

Response : As one new panel has been inserted in Figure 2, a new figure caption is given, taking into account the comments of the Reviewer. Here is what we propose:

"Cloud-to-ground lightning climatology in terms of number of days with at least one cloud-to-ground lightning flash recorded per day in a regular grid of 5km x 5km and cumulated over the period investigated as sensed by Météorage from 1997 to 2012 (a), contribution of the 2012 records expressed in % relative to the 1997–2012 number of days per 5km x 5km pixel (b), and number of days per year (c) for the period September–November 2012 between over South East of France. The red solid line plotted in (c) corresponds to the average value for the 1997-2012 period. Red and dark red lines indicate 200m and 1000m height, respectively. The Cévennes-Vivarais domain is also delimited by the black polygon."

- What is written in between brackets '(about 0.3% ... climatology)' should be written in the text and not in the caption of the figure.

Response : It has been removed from the caption and is now inserted in the manuscript in the paragraph describing Figure 2.

Fig. 6: - Bolt-from-the-blue

Response : Corrected.

Fig. 8:

- rewrite: '...recorded during between ...'

Response : We removed "during".

- (g): ...'available only for EUCLID and LINET with ...': I see black stars for ZEUS as well

Response : The type of strokes is only available from EUCLID and LINET. This information does not exist for ZEUS. To avoid any mis-understanding, we removed the part of the sentence "and type of detected events available only for EUCLID and LINET".

Fig. 9: Figures are too small to see

Response : The figures were plotted per day and provided individually for the typesetting. The original size of daily-based figures is about the size of Figure 3.

1 **An overview of the lightning and atmospheric electricity observations collected in**  
2 **Southern France during the HYdrological cycle in Mediterranean EXperiment**  
3 **(HyMeX), Special Observation Period 1**

4  
5 Authors : Eric Defer (LERMA, UMR8112, CNRS-OP-ENS-UPMC-UCP), Jean-Pierre Pinty (LA,  
6 UMR5560, Université de Toulouse & CNRS), Sylvain Coquillat (LA, UMR5560, Université  
7 de Toulouse & CNRS), Jean-Michel Martin (LA, UMR5560, Université de Toulouse &  
8 CNRS), Serge Prieur (LA, UMR5560, Université de Toulouse & CNRS), Serge Soula (LA,  
9 UMR5560, Université de Toulouse & CNRS), Evelyne Richard (LA, UMR5560, Université  
10 de Toulouse & CNRS), William Rison (NMT), Paul Krehbiel (NMT), Ronald Thomas  
11 (NMT), Daniel Rodeheffer (NMT), Christian Vergeiner (Technische Universität Graz),  
12 François Malaterre (Météorage), Stéphane Pedeboy (Météorage), Wolfgang Schulz  
13 (ALDIS), Thomas Farges (CEA, DAM-DIF), Louis-Jonardan Gallin (CEA, DAM-DIF),  
14 Pascal Ortéga (UPF), Jean-François Ribaud (CNRM-GAME, UMR3589, Météo-France &  
15 CNRS), Graeme Anderson (UK Met Office), Hans-Dieter Betz ([Nowcast GmbH](#)), Baptiste  
16 Meneux ([Nowcast GmbH](#)), Vassiliki Kotroni (NOA), Kostas Lagouvardos (NOA), Stéphane  
17 Roos (Météo France), Véronique Ducrocq (CNRM-GAME, UMR3589, Météo-France &  
18 CNRS), Odile Roussot (CNRM-GAME, UMR3589, Météo-France & CNRS), Laurent  
19 Labatut (CNRM-GAME, UMR3589, Météo-France & CNRS), Gilles Molinié (LTHE)

20  
21  
22 Submitted to AMTD – Revised version  
23 (with corrected text and updated figures only)

24  
25  
26 Corresponding Author: Eric Defer (LERMA)  
27 [eric.defer@obsppm.fr](mailto:eric.defer@obsppm.fr)  
28 LERMA – CNRS/Observatoire de Paris  
29 61 avenue de l'Observatoire  
30 75014 Paris  
31 France  
32 +33 1 40 51 21 35  
33  
34

34  
35  
36  
37  
38  
39  
40  
41  
42  
43  
44  
45  
46  
47  
48  
49  
50  
51  
52  
53  
54  
55

**Abstract:**

The PEACH [project](#) (Projet en Electricité Atmosphérique pour la Campagne HyMeX -- the Atmospheric Electricity Project of HyMeX Program) is the Atmospheric Electricity component of the HyMeX (Hydrology cycle in the Mediterranean Experiment) experiment and is dedicated to the observation of both lightning activity and electrical state of continental and maritime thunderstorms in the area of the Mediterranean Sea. During the HyMeX SOP1 (Special Observation Period) [from 5 September to 6 November 2012](#), four European Operational Lightning Locating Systems (OLLSs) ([ATDnet](#), EUCLID, LINET, ZEUS) and the HyMeX Lightning Mapping Array network (HyLMA) were used to locate and characterize the lightning activity over the Southeastern Mediterranean at flash, storm and regional scales. Additional research instruments like slow antennas, video cameras, micro-barometer and microphone arrays were also operated. All these observations in conjunction with operational/research ground-based and airborne radars, rain gauges and in situ microphysical records aimed at characterizing and understanding electrically active and highly precipitating events over Southeastern France that often lead to severe flash floods. Simulations performed with Cloud Resolving Models like Meso-NH and WRF are used to interpret the results and to investigate further the links between dynamics, microphysics, electrification and lightning occurrence. [Herein we present an overview of the PEACH project and its different instruments. Examples are discussed to illustrate the comprehensive and unique lightning dataset, from radio-frequency to acoustics, collected during the SOP1 for lightning phenomenology understanding, instrumentation validation, storm characterization and modeling.](#)

## 55 1-Introduction

56

57 A lightning flash is the result of an electrical breakdown occurring in an electrically charged cloud.  
58 Charged regions inside the cloud are created through electrification processes, dominated by ice-ice  
59 interactions. Electrical charges are exchanged during rebounding collisions between ice particles of  
60 different nature in the presence of supercooled water. This corresponds to the most efficient non-inductive  
61 charging process investigated by Takahashi (1978) and Saunders et al. (1991). Laboratory studies have  
62 shown that the transfer of electrical charges between ice particles in terms of amount and sign is very  
63 complex and depends on the difference of velocity between the two [ice particles, temperature and liquid](#)  
64 [water content](#). The lighter hydrometeors are transported upward, the heaviest being sustained at lower  
65 altitude in the cloud. Combined with cloud dynamics and cloud microphysics, electrification processes  
66 lead to dipoles, tripoles and even stacks of charged zones vertically distributed in the thundercloud  
67 (Stolzenburg et al., 1998; Rust et al., 2005). Between the charged regions, the ambient electric field can  
68 reach very high values, i.e. more than one hundred  $\text{kV m}^{-1}$  (Marshall et al., 2005). [However, such an](#)  
69 [electric field intensity is of one order](#) of magnitude lower than the electric field threshold required to  
70 breakdown cloud air. Therefore, additional ignition mechanisms have been considered such as runaway  
71 electrons (Gurevich et al., 1992) or hydrometeor interactions [present in](#) with high electric fields (Crabb and  
72 Latham, 1974; Coquillat and Chauzy, 1994; Schroeder et al., 1999; Coquillat et al., 2003). Natural  
73 lightning flashes then occur when the ambient electric field exceeds a threshold [of a few kV/m. Hence, it is](#)  
74 [clear that](#) the lightning activity of a thundercloud results from intricate and complex interactions between  
75 microphysical, dynamical and electrical processes.

76 Lightning flashes are usually classified into two groups: Intra-Cloud (IC) flashes only occur in  
77 [cloud, while](#) Cloud-to-Ground (CG) flashes connect to the ground. Negative (positive) CG flashes lower  
78 negative (positive) [charge](#) to the ground and exhibit significant electromagnetic [when connecting the](#)  
79 [ground](#). Negative CG flashes are more frequent than positive CG flashes, and generally occur with  
80 multiple connections to the ground ([e.g. Mäkelä et al. \(2010\), Orville et al. \(2011\)](#)). Positive CG flashes  
81 are relatively rare and often composed of a single or very few connections to the ground with higher  
82 current than negative CG flashes. A natural lightning flash is not a continuous phenomenon but is in fact

83 composed of successive events, also called flash components, with different physical properties in terms  
84 of discharge propagation, radio frequency radiation type, current properties, space and time scales. A  
85 lightning flash is then constituted of a series of multi-scale physical processes spanning from the electron  
86 avalanche to the propagation of discharges over large distances of a few km or more. Each of these sub-  
87 processes radiates electromagnetic waves in a wide wavelength spectrum.

88 Different detection techniques have been developed to detect and locate these processes. They  
89 usually operate at specific wavelength ranges and are sensitive to some components of the lightning  
90 discharges. For instance, some ground-based or space borne sensors detect electromagnetic radiation  
91 emitted in the Very High Frequency (VHF) domain (e.g. Proctor, 1981; Shao and Krehbiel, 1996;  
92 Jacobson et al., 1999; Krehbiel et al., 2000; Defer et al., 2001; Defer and Laroche, 2009). Other  
93 instruments detect the radiation emitted by lightning flashes in the optical wavelength (e.g. Light et al.,  
94 2001; Christian et al., 2003) or in the Very Low Frequency/Low Frequency (VLF/LF) range (e.g. Cummins  
95 et al., 1998; Smith et al., 2002; Betz et al., 2008, 2009). But because no technique covers all the physical  
96 aspects of a lightning flash, multi-instrumental observations are required to provide the most  
97 comprehensive description in order to analyze in great detail the lightning flashes and consequently the  
98 whole lightning activity of a thunderstorm.

99 Lightning flashes can be investigated flash-by-flash to derive their properties. With appropriate  
100 lightning sensors such as VHF lightning mappers, the temporal and spatial evolution of the lightning  
101 activity can be related to the characteristics of the parent clouds. The total (IC+CG) flash rate is usually a  
102 good indicator of the severity of convective systems (Williams et al., 1999). A sudden increase (decrease)  
103 of the flash rate is often associated to a more vigorous convection (storm decay). Flash rates usually  
104 increase while the storm is developing because conditions for a significant non-inductive charging process  
105 are favorable. Flash rates reach a peak value when the cloud top reaches its maximum altitude and then  
106 decreases at the onset of the decaying stage of the parent thundercloud. Links between severe weather  
107 phenomena including lightning flashes, tornadoes, hail storms, wind gusts, flash floods have been studied  
108 since many years. As IC observations were not widely recorded and disseminated, numerous  
109 investigations used CG reports to predict severe weather (e.g. Price et al., 2011; Kohn et al., 2011).  
110 However, in the past decade it has been shown that the total lightning activity is a more reliable indicator

111 of severe weather (e.g. MacGorman et al., 1989; Goodman et al., 1998; Williams et al., 1999; Montanyà et  
112 al., 2007). Schultz et al. (2011) report indeed that the use of total lightning trends is more effective than  
113 CG trends to identify the onset of severe weather with an average lead time prior to severe weather  
114 occurrence higher when total lightning detection is used as compared to CG detection only. Because  
115 detection of the electromagnetic lightning signal can be instantaneously recorded, located and analyzed,  
116 flash rate, IC/CG ratio, vertical distribution of the lightning activity, flash duration and flash density can be  
117 used to identify in real time severe weather but deeper investigations are required.

118         Having illustrated the potential advantages and the difficulties arising from lightning-storm severity  
119 relationships, it is useful to review some available modeling tools to investigate this issue. Among them, 3-  
120 D Cloud Resolving Models (CRM) including parameterizations of both electrification mechanisms and  
121 lightning discharges are of highest interest. For instance, Mansell et al. (2002) included a very  
122 sophisticated lightning flash parameterization in the electrification model of Ziegler et al. (1991). Poeppl  
123 (2005) also improved a lightning parameterization in the pioneering model of Helsdon et al. 1987, 2002).  
124 On their side Altaratz et al. (2005) concentrated their efforts to test a storm electrification scheme in a  
125 regional model (RAMS) but without simulating the lightning flashes, which constitutes by far the most  
126 difficult part. More recently, Yair et al. (2010) have developed a method for predicting the potential for  
127 lightning activity based on the dynamical and the microphysical fields of Weather Research and  
128 Forecasting (WRF) model. Cloud electrification and discharge processes have also been included recently  
129 in the French community model Meso-NH (Molinié et al., 2002; Barthe et al., 2005, 2007; Barthe and Pinty,  
130 2007a, b).

131         CRMs are the preferred modeling tools to study the sensitivity of the electrical charge structure to  
132 the electrification mechanisms (see Barthe et al., 2007a, b). A key challenge in simulating cloud  
133 electrification mechanisms is the lack of agreement in the community about the relevance of each of the  
134 non-inductive charging diagrams published by Takahashi (1978) and by Saunders et al. (1991). Those  
135 diagrams disagree in some way because the protocol of the laboratory experiments was different. As a  
136 consequence, changing the non-inductive parameterization rates according to these diagrams deeply  
137 modifies the simulated cloud charge structure where regular dipole, inverse dipole or tripole of charge  
138 layers can be obtained while keeping the same microphysics and dynamics in the CRMs.

139 Lightning detection is definitively useful to monitor thunderstorms and to help improve severe  
140 weather simulations. Among the open scientific questions related to the electrical activity, are the links  
141 between microphysics, kinematics and lightning activity, the use of the lightning information in multi-  
142 sensor rainfall estimation and the lightning-flash phenomenology. In the following we describe the  
143 rationale for dedicated lightning observations to characterize the electrical properties of Northwestern  
144 Mediterranean storms during a dedicated campaign of the HYdrological cycle in the Mediterranean  
145 EXperiment (HyMeX) program (Ducrocq et al., 2013). First, the HyMeX project is briefly described in Sect.  
146 2. The scientific questions and the observational strategy of the HyMeX lightning task team, including  
147 instruments and models, are described in Sect. 3. Section 4 presents an overview of the observations  
148 collected at flash, storm and regional scales. Section 5 then discusses the perspectives by listing out the  
149 next steps of the data analysis as well as the data and products made available to the HyMeX  
150 Community.

151

## 152 **2-The HyMeX program**

153

154 The Mediterranean region is regularly affected by heavy precipitation often causing devastating  
155 flash-floods. Floods and landslides in the Mediterranean Basin cost lives and lead to expensive property  
156 damage. Improving the knowledge and forecast of these high-impact weather events is a major objective  
157 of the HyMeX program (Ducrocq et al., 2013). As part of this 10-year program, the first Special  
158 Observation Period (SOP1) HyMeX field campaign was conducted during 2 months from 5 September  
159 2012 to 6 November 2012 over Northwestern Mediterranean Sea and its coastal regions in France, Italy,  
160 and Spain. The instrumental and observational strategy of the SOP1 campaign was set up to document  
161 and improve the knowledge on atmospheric processes leading to heavy precipitation and flash flooding in  
162 that specific Mediterranean region. A large battery of atmospheric research instruments were operated  
163 during the SOP1 including among others mobile weather Doppler and polarimetric radar, airborne radar,  
164 in situ microphysics probes, lidar, and rain gauges (Ducrocq et al., 2013; Bousquet et al., 2014). Those  
165 equipments were deployed at or near super sites where dedicated research instruments are gathered to  
166 document specific atmospheric processes (Ducrocq et al., 2013). The research lightning sensors operated

167 during the HyMeX SOP1 were located in the [Cévennes-Vivarais](#) (CV) area in Southeastern France.  
168 [Additionally, various](#) operational weather forecasting models were used as detailed in Ducrocq et al.  
169 (2013).

170 The HyMeX program (Ducrocq et al., 2013) and its intensive observation period of autumn 2012  
171 was an interesting opportunity to implement multi-instrumental observations for documenting the various  
172 processes related to electrification of thunderstorms in a region prone to thunderstorms and high  
173 [precipitating events](#). This was performed during the PEACH (Projet en Electricité Atmosphérique pour la  
174 Campagne HyMeX -- the Atmospheric Electricity Project of HyMeX Program) experiment, the HyMeX  
175 Atmospheric Electricity component as detailed in the following.

176

### 177 **3-The PEACH experiment**

178

179 Summer electrical activity is predominately located over continental Europe while during winter the  
180 electrical convective clouds are mainly observed over the Mediterranean Sea as established by  
181 climatology based on lightning records (e.g. Holt et al., 2001; Christian et al., 2003; Defer et al., 2005) or  
182 on space-based microwave measurements (e.g. Funatsu et al., 2009). Holt et al. (2001) discussed that  
183 the largest number of days with thunderstorms over the Mediterranean Basin is located near the coasts of  
184 Italy and Greece. Based on 3-year Tropical Rainfall Measurement Mission (TRMM) Lightning Imaging  
185 Sensor (LIS) observations, Adamo (2004) reported that the flash rates over the Mediterranean Sea as  
186 deduced from LIS are significantly smaller than those recorded at similar latitudes in the United States.  
187 This finding is consistent with the fact that convection and consequently lightning activity are significantly  
188 stronger over land than over sea (Christian et al., 2003).

189 Current geostationary [satellites](#) can offer a relatively satisfying revisiting time (15 min) to track the  
190 storms but cannot provide sounding information below the cloud top. Space-based passive and active  
191 microwave sensors on low orbit satellite missions such as TRMM (Kummerow et al., 1998) or A-Train  
192 (Stephens et al., 2002) only provide a scientifically relevant snapshot of the sampled clouds, but the ability  
193 of low orbit instruments to monitor and track weather systems is very limited. Lightning detection data from  
194 ground-based detection networks is available continuously and instantaneously over the continental and

195 maritime Mediterranean area as detailed in the following. Lightning information can monitor severe  
196 weather events over continental and maritime Mediterranean region but can also improve weather  
197 forecast with lightning data assimilation (Lagouvardos et al., 2013). However, further scientific  
198 investigations are required to document the links between the lightning activity and the dynamical and  
199 microphysical properties of the parent clouds in continental and maritime Mediterranean storms. In  
200 addition it is necessary to identify the key parameters derived from OLLS records alone or in combination  
201 with other meteorological observations to provide suitable proxies for a better storm tracking and  
202 monitoring over the entire Mediterranean Basin.

203

### 204 **3.1 Scientific objectives and observational/modeling strategy**

205

206 In the frame of the HyMeX program, several international Institutes joined their effort to investigate  
207 the lightning activity and the electrical state of thunderstorms. This topic is part of the HyMeX Working  
208 Group WG3 dedicated to the study of heavy precipitation events (HPEs), flash-floods and floods. The  
209 PEACH team, composed of the Authors of the present article, identified five observational- and modeling-  
210 based scientific objectives in relation to HyMeX goals:

- 211 i) Study the relationships between kinematics, microphysics, electrification, aerosols and lightning  
212 occurrence and characteristics,
- 213 ii) Document the electrification processes and charge structures inside clouds over sea and land, and  
214 during sea-to-land and land-to-sea transitions,
- 215 iii) Promote the use of lightning records for data assimilation, nowcasting and very short range  
216 forecasting applications,
- 217 iv) Cross-evaluate lightning observations from different OLLSs,
- 218 v) Establish climatology of lightning activity over the Mediterranean Basin.

219 The first three scientific objectives exhibit obvious connections with WG3 objectives to document  
220 and understand thunderstorms leading to HPEs and flash-floods and to explore the pertinence of lightning  
221 detection in conjunction or not with operational weather observations to improve monitoring and  
222 forecasting of the storm activity. The fourth objective focuses on the inter-comparison of OLLS records as

223 lightning [detection with a quasi instantaneous data delivery to the users](#), and geostationary imagery are  
224 the only two weather observing techniques readily available over the full Mediterranean Basin. The fifth  
225 objective aims at documenting long-term series of lightning-based proxies of thunderstorms during the  
226 10\,year duration of the HyMeX program but also from more than 2 decades of past lightning data  
227 available from some European OLLSs.

228         The PEACH observational strategy followed the HyMeX observational strategy with SOP (Special  
229 Observation Period), EOP (Enhanced Observation Period) and LOP (Long Observation Period) activities.  
230 SOP1 activities are mainly described here while EOP and LOP are briefly discussed as they are still  
231 underway at the time of the writing. The SOP1 PEACH strategy consisted in deploying a relevant  
232 instrumentation from September to November 2012 in key locations together with instruments operated by  
233 other HyMeX teams with common temporal and spatial coverage over the [Cévennes-Vivarais \(CV\)](#)  
234 domain. First, OLLSs with continuous, good quality coverage of the Mediterranean were identified. Then  
235 a total-lightning detection system was considered and a portable Lightning Mapping Array (HyLMA) was  
236 selected. Electric field mills (EFMs), slow antennas ([SLAs](#)), as well as induction rings (INRs) were also  
237 listed as key instruments for characterizing the ambient electric field, the change of the electric field  
238 induced by the lightning occurrence, and the electrical charges carried by raindrops at ground level,  
239 respectively. [Finally, in](#) order to increase the scientific returns, additional research field instruments were  
240 operated, including a mobile optical camera combined with electric field measurement (VFRS, Video and  
241 Field Record System), micro-barometer and micro-phone arrays ([MBA and MPA, respectively](#)) and  
242 Transient Luminous Event (TLE) cameras (Fullekrug et al., 2013). [The PEACH project also includes](#)  
243 [two cloud resolving models, MesoNH with its electrification and lightning scheme, and WRF.](#)

244         As discussed in Duffourg and Ducrocq (2011) and Ducrocq et al. (2013), the Southeastern part of  
245 France has experienced in the past heavy precipitation with devastating flash-floods, floods and  
246 landslides. The PEACH observational setup in conjunction with the other HyMeX research and operational  
247 instrumentation aims at documenting the lightning activity existing, or not, in those heavy precipitation  
248 systems. The HyLMA observations combined with the OLLS records provide the required accurate  
249 description of the lightning activity (e.g. flash rate, flash density, IC/CG ratio, vertical and horizontal flash  
250 development) to investigate its relationships with the dynamical and microphysical cloud properties [in](#)

251 combination with ground-based and airborne radars and in situ measurements. Such investigation is the  
252 basis to develop new lightning-based tools for nowcasting and very short range forecasting applications.  
253 In addition, the HyLMA observations, in conjunction or not with ground-based electric field measurements,  
254 help to investigate the temporal and spatial evolution of the charge structures inside the clouds, over sea  
255 and land, as deduced from the properties of the VHF signal radiated by the different flash components.  
256 The capability to map with HyLMA the three-dimensional structure of the lightning flashes, as well as the  
257 regions of electrical charges in the thunderclouds allows the validation of lightning/electrification schemes  
258 implemented in numerical cloud resolving models and the investigation of new lightning data assimilation  
259 schemes. Finally, to establish a solid climatology of lightning activity over the Mediterranean Basin from  
260 more than 2 decades of OLLS records, the study of concurrent HyLMA, OLLSs and VFRS records is  
261 required not only to access the actual performances of the OLLSs but also to determine precisely the flash  
262 components that OLLSs record in the perspective of a better operational use of OLLS observations.

263 As a result, the HyMeX SOP1 experiment is probably the first ambitious field experiment in  
264 Europe to offer such comprehensive description of lightning activity and of its parent clouds over a  
265 mountainous area from the early stage to the decaying phase of the sampled electrical storms. Note that a  
266 battery of ground-based and airborne research radars in conjunction with the operational network of  
267 Météo-France provided a detailed description of the thunderclouds as detailed in Bousquet et al. (2014).  
268 Other instruments were deployed as listed in Ducrocq et al (2013). In this article we give some examples  
269 of only atmospheric electricity observations. Several studies are underway on the electrical properties of  
270 thunderstorms relatively to cloud properties like cloud structure, microphysics and rain patterns as derived  
271 from radar and satellite observations and in situ measurements.

272

### 273 **3.2 Research instruments deployed during the SOP1**

274

#### 275 **3.2.1 The HyMeX Lightning Mapping Array (HyLMA)**

276

277 A twelve station Lightning Mapping Array (Rison et al., 1999; Thomas et al., 2004) was deployed  
278 in the HyMeX SOP1 area from spring to autumn of 2012 (Fig. 1). The HyLMA stations, located in RF-

279 quiet, mainly rural areas, were solar powered and used broadband cell-phone modems for  
280 communications. Each HyLMA station recorded the arrival times and amplitudes of the peaks of impulsive  
281 VHF sources, recording at most one peak in every 80- $\mu$ s interval. Locations of impulsive VHF sources  
282 were determined by correlating the arrival times for the same event at multiple stations (Thomas et al.,  
283 2004). Every minute, a subset of the raw data (the peak in every 400- $\mu$ s interval) was transferred to a  
284 central computer for real-time processing and display. The full data was retrieved at the end of the project  
285 for more complete post-processing.

286 An LMA locates the strongest VHF source in every 80- $\mu$ s interval. Because negative leaders  
287 radiate much more strongly than positive leaders, and because negative and positive leaders typically  
288 propagate at the same time, an LMA primarily locates lightning channels from negative leaders. In  
289 particular, an LMA rarely detects the positive leaders from positive cloud-to-ground strokes.

290 The HyLMA detected all lightning over the array with a location accuracy of about 10 m  
291 horizontally and 30 m vertically (Thomas et al., 2004). The HyLMA located much of the lightning outside  
292 of the array, with increasingly large location errors (< 1 km at 200 km range) out to a distance of about 300  
293 km from the array center. In order to locate a source, at least six stations must have line-of-sight to that  
294 source. The lines-of-sight of most of the stations to low-altitude lightning channels outside of the array  
295 were blocked by the mountainous terrain in Southeastern France, so the LMA typically detected only the  
296 higher altitude lightning channels outside the array.

297

### 298 **3.2.2 Slow Antennas (SLAs)**

299

300 Two solar-powered slow antennas were deployed to measure the electrostatic field changes from  
301 lightning in the SOP1 area. One SLA was deployed a few tens of meters from the Micro-Barometer and  
302 Microphone Arrays (MBA/MPA, see Sect. 3.2.3) near the Uzès airfield, and the second was deployed near  
303 the HyLMA station at the Grand Combe airfield. Each SLA consisted of an inverted flat-plate antenna  
304 connected to a charge amplifier with a 10-s decay constant. The output of the charge amplifier was  
305 digitized at a rate of 50,000 samples per second with a 24-bit A/D converter, synchronized to a local GPS  
306 receiver, and the data were recorded continuously on SD cards.

307

308

### 3.2.3 The Micro-barometer and Microphone Arrays (MBA/MPA)

309

310

311

312

313

314

315

The CEA (Commissariat à l'Energie Atomique) team installed two arrays, which overlapped each other: a micro-barometer array (MBA) and a microphone array (MPA). The MBA was composed of four MB2005 micro-barometers arranged in an equilateral triangle of about 500 m side with one at the barycenter of the triangle while the MPA was composed of four microphones arranged in an equilateral triangle of about 52 m side with one at the barycenter of the triangle. The MBA and MPA barycenters were localized at the same place.

316

317

318

319

320

321

322

323

324

Each sensor measures the pressure fluctuation relative to the absolute pressure. The MB2005 microbarometer has a sensitivity of a few millipascals through a band pass of 0.01–27 Hz. This sensor is used in most of the infrasound stations of the International Monitoring System of the Comprehensive nuclear Test Ban Treaty Organization ([www.ctbto.org](http://www.ctbto.org)). The microphone is an encapsulated BK4196 microphone. Its sensitivity is about 10 mPa through a band pass of 0.1 – 70 Hz. In order to minimize the noise due to surface wind effects, each sensor is connected to a noise reducing system equipped with multi-inlet ports (8 for the microbarometers and 4 for the microphones) that significantly improves the detection capability above 1 Hz. To further reduce the wind noise, micro-barometers were installed under vegetative cover (i.e. pine forest).

325

326

327

328

329

The signal of these sensors was digitalized at 50 Hz for the MBA and 500 Hz for the MPA. The dating was GPS tagged. Data were stored on a hard disk. No remote access was possible during the SOP1. To avoid power blackouts, each measurement point was supplied with 7 batteries. Those batteries needed to be recharged at the middle of the campaign, meaning that the MBA and MPA were unavailable from 9 to 12 October.

330

331

332

333

334

The data from each sensor of the arrays were compared using cross-correlation analysis of the waves recorded. The azimuth and the trace velocity were calculated for each detected event when a signal was coherent over the array. Using the time of the lightning discharge and these parameters, a 3-D location of acoustic sources generated by the thunder is possible (e.g. Farges and Blanc, 2010; Arechiga et al., 2011; Gallin, 2014). Gravity waves generated by thunderstorms (Blanc et al., 2014), could also be

335 monitored by MBA. When a convective system goes over an array, a large pressure variation is  
336 measured.

337

### 338 **3.2.4 Electric Field Mills (EFM)**

339

340 The surface electrostatic field can be used to detect the presence of charge overhead within a  
341 cloud. This parameter is generally measured with a field mill and the value obtained can be very variable  
342 according to the sensor shape and location, the relief of the measurement site, the nature of the  
343 environment, *etc.* The field value and its evolution must be interpreted very carefully due to the variety of  
344 sources of charge: the cloud charge, the space charge layer which can develop above ground from  
345 corona effect on the ground *irregularities*, and the charge carried by the rainfall (Standler and Winn, 1979;  
346 Chauzy et al., 1987; Soula et al., 2003). However, the electric field evolution can be used to identify  
347 discontinuities due to the lightning flashes, which can be related to the flashes detected by location  
348 systems (Soula and Georgis, 2013).

349 The field-mills used in three of the stations were Previstorm models from Ingesco Company and  
350 were initially used in Montanya et al. (2009). The measurement head is *oriented* downward to avoid rain  
351 disturbances, and is fixed at the top of a 1-meter mast that reinforces the electrostatic field on the  
352 measuring electrode. The measuring head of the fourth field-mill was orientated upward and flush to the  
353 ground thanks to a hole dug in the ground. The field mills were calibrated by using a shielding to have  
354 zero and by considering the fair weather conditions that correspond to the theoretical value of  $130 \text{ V m}^{-1}$ .  
355 The data from each sensor was recorded with a time resolution of 1 s. This time resolution readily reveals  
356 the major discontinuities in the electrostatic field caused by the lightning flashes without the distracting  
357 effects of much faster individual processes within a flash. *The polarity of the field is positive when the field  
358 points upward and the electric field is created by negative charge overhead.*

359

### 360 **3.2.5 Induction Ring (INR)**

361

362           The electric charge carried by raindrops can easily be detected and measured by a simple  
363 apparatus commonly called induction ring. This sensor is constituted of a cylindrical electrode (the ring) on  
364 the inner surface of which induced electric charges appear by electrostatic influence when a charge  
365 raindrop enters the sensor. When the drop leaves the sensor, the induced charges disappear. The  
366 cylindrical electrode is connected to an electrometer and the current signal induced by the passing of a  
367 charged drop (a bipolar current impulse) is sampled at a rate of 2000 Hz. It is amplified and integrated by  
368 an electronic circuitry that directly provides the charge signal. This one appears as a single pulse with  
369 amplitude and length proportional to the charge and to the velocity of the drop, respectively. The actual  
370 charge is deduced from the calibration of the sensor. If the drop collides with the induction cylinder, the  
371 pulse signal exhibits a slow exponential decay (MacGorman and Rust, 1998) that is easily recognizable in  
372 the post data processing. In this case, the raindrop charge that is fully transferred to the induction cylinder  
373 is determined by a specific calibration. The charge measurement sensitivity ranges from about  $\pm 2$  pC to  $\pm$   
374 400 pC. Furthermore, the charge signal duration at mid height can be used to determine the size of the  
375 charged raindrops provided the relationship between size and fall velocity in function of the actual  
376 temperature and pressure (Beard, 1976).

377           Such measurement provides key information on the electric charge carried by the rain at the  
378 ground to validate numerical modeling. It documents the spectrum of charged drops and helps deduce the  
379 proportion of charged drops within the whole drop population by comparing its spectrum with the one  
380 measured by a disdrometer. Four induction rings were built and operated during the SOP1, mainly along  
381 the South to North axis at the foothills of the Massif Central where most of high precipitating events occur.  
382 Unfortunately, only few events passed above the sensors and in these rare cases, the main electronic  
383 component of the induction rings suffered dysfunction that were not detected during the laboratory tests,  
384 so no valuable INR data are available for the SOP1.

385

### 386           **3.2.6 Video and Field Recording System (VFRS)**

387

388           The VFRS instrument is a transportable system used to measure electric fields and to record high-  
389 speed videos at various locations. The calibrated E-field measurement consists of a flat plate antenna, an

390 integrator-amplifier, a fiber optic link and a digitizer. The bandwidth of the E-field measurement was in the  
391 range from about 350Hz to about 1MHz. A 12-bit digitizer with a sampling rate of  $5 \text{ MS.s}^{-1}$  was used for  
392 data acquisition. The high-speed camera was operated at 200 fps (equivalent to an exposure of 5  
393 ms/frame),  $640 \times 480$  pixel and 8 Bit grayscale resolution. The GPS clock provided an accurate time  
394 stamp for the E-field and the video data. The range of the VFRS was mainly dependent on the visibility  
395 conditions. At adequate visibility, combined video and electric field data could record up to distances of  
396 about 50 km with sufficient quality. The VFRS was transportable with a car and independent of any  
397 external power supply. Detailed description of the used VFRS can be found in Schulz et al. (2005) and in  
398 Schulz and Saba (2009). For the typical observations during SOP1, the VFRS was operated in the manual  
399 trigger mode using an adjustable pre- and post-trigger. To ensure capturing the entire lightning discharge  
400 we typically recorded 6 s of data with 2 s of pre-trigger data per observed flash. During some storms (e.g.  
401 low visibility conditions), the VFRS was operated in the continuous recording mode. Due to memory  
402 limitations we only recorded the electric fields in the continuous recording mode.

403 All observation days during SOP1 were chosen based on weather forecasts with sufficient  
404 thunderstorm risk over the region of interest. As the real situation could be different to the forecast  
405 scenario, e.g. location, motion and stage of the storms, the VFRS sometimes had to be moved from the  
406 initial site to another one. For each field operation the lightning activity of the targeted thunderstorm was  
407 monitored in real time using EUCLID and HyLMA observations. The VFRS was often deployed at several  
408 sites during a typical observation day. An observation day was finished when no more thunderstorms  
409 were expected to occur.

410

### 411 **3.2.7 Locations and status of the research instruments**

412

413 Figure 1 presents the locations of the different PEACH instruments operated during SOP1. The  
414 HyLMA network consisted in a dense 8-station network more or less centered on Uzès (Gard) with 4  
415 additional remote stations located on the western side of the CV domain. SLA antennas were deployed in  
416 two different locations: one at the center of the HyLMA network few tens of meters away from MPA and  
417 MBA, the second one in the hills few hundreds meters away from Grand Combe HyLMA station (Table 1).

418 INR and EFM were installed on the same sites with other HyMeX SOP1 instruments like rain gauge,  
419 video-distrometers and MRRs (Micro Rain Radar; Bousquet et al., submitted to BAMS). VFRS  
420 observations were performed at different locations during the SOP1 according to the forecast and the  
421 evolution of the storm activity with guidance from HyMeX Operation Center and members of the lightning  
422 team. Finally, the four OLLSs continuously covered the entire SOP1 domain.

423 Table 2 shows the status of the instruments during the SOP1 period and after its completion.  
424 HyLMA was initially operated with 6 stations starting on 1 June 2012. HyLMA was then operated with 11  
425 stations starting early August 2012. The 12<sup>th</sup> HyLMA station was online early beginning of September  
426 2012. Low time resolution (400- $\mu$ s time window) HyLMA lightning observations were delivered in real time  
427 during the SOP1 period through wireless communication and displayed on the HyMeX Operation Center  
428 web site as well as on a dedicated server at NMT. The full HyLMA data were reprocessed after the  
429 completion of the SOP1 campaign and only high temporal resolution HyLMA data are used in the analysis  
430 and distributed to the HyMeX Community. Additionally, ATDnet, EUCLID and ZEUS observations were  
431 also delivered in real time to the HyMeX Operation Center.

432

### 433 **3.3 Operational Lightning Locating Systems**

434

#### 435 **3.3.1 ATDnet**

436

437 The UK Met Office VLF ATDnet (Arrival Time Differencing NETWORK) lightning location network  
438 takes advantage of the long propagation paths of the VLF (frequency range) sferics emitted by lightning  
439 discharges, which propagate over the horizon via interactions with the ionosphere (Gaffard et al., 2008).  
440 The ATDnet network consists of 11 that regularly contribute to the “operational network”, plus sensors  
441 distributed further afield. The waveforms of VLF sferics received at the ATDnet sensors are transmitted to  
442 a central processor in Exeter, where the waveforms are compared in order to estimate arrival time  
443 differences. These arrival time differences are compared with theoretical arrival time differences for  
444 different locations, in order to estimate the most likely source location. Current ATDnet processing  
445 requires four ATDnet sensors to detect a lightning stroke in order to be able to calculate a single,

446 unambiguous source location. ATDnet predominantly detects sferics created by CG strokes, as the  
447 energy and polarization of Sferics created by CG return strokes can travel more efficiently in the Earth–  
448 Ionosphere waveguide, and so are more likely to be detected at longer ranges than typical IC discharges.  
449 ATDnet location uncertainties within the region enclosed by the network of sensors are on the order of a  
450 few kilometers, i.e. suitable for identifying electrically active cells.

451

### 452 **3.3.2 EUCLID**

453

454 The EUCLID network (EUropean Cooperation for LIghtning Detection) is a cooperation of several  
455 European lightning detection networks (Austria, Finland, France, Germany, Italy, Norway, Portugal,  
456 Slovenia, Spain, and Sweden) that operate state-of-the-art lightning sensors. As of August 2009 the  
457 EUCLID network employs 137 sensors, 5 LPATS III, 18 LPATS IV, 15 IMPACT, 54 IMPACT ES/ESP, 3  
458 SAFIR and 42 LS7000 sensors (oldest to newest), all operating over the same frequency range (1 kHz -  
459 350 kHz) with individually-calibrated gains and sensitivities. Data from all of these sensors are processed  
460 in real-time using a single common central processor, which also produces daily performance analyses for  
461 each of the sensors. This assures that the resulting data are as consistent as possible throughout Europe.  
462 In fact, the Europe-wide data produced by EUCLID is frequently of higher quality than the data produced  
463 by individual country networks, due to the implicit redundancy produced by shared sensor information.  
464 Since the beginning of the cooperation the performance of the EUCLID network has been steadily  
465 improved, e.g. with improved location algorithms, with newer sensor technology and by adapting sensor  
466 positions because of bad sites. The flash/stroke detection efficiency (DE) of the EUCLID network in the  
467 south of France was determined to be 90%/87% for negative and 87%/84% for positive discharges but for  
468 a time period where a close sensor was out of order (Schulz et al., 2014). Therefore the values should be  
469 rated as lower limits of EUCLID DE in this region. The location accuracy was determined to be 256 m but  
470 based on 14 strokes only.

471

### 472 **3.3.3 LINET**

473

474

475           The LINET system is a modern lightning detection network in the VLF/LF domain (5 kHz – 100  
476 kHz) developed by nowcast GmbH (Betz et al., 2008, 2009). LINET Europe consists of more than 120  
477 sensors placed in 25 countries. Each of them includes a field antenna, a GPS antenna and a field  
478 processor. The field antenna measures the magnetic flux produced by a lightning. The processor  
479 evaluates this signal and combines it with the accurate time provided by the GPS antenna. Compact data  
480 files are then sent to a central processing unit where the final stroke solutions are generated. Accurate  
481 location of strokes requires that the emitted signal is detected by many sensors. Reported strokes are  
482 based on reports from at least 5 sensors. Strokes are located using the Time-Of-Arrival (TOA) method.  
483 LINET detects also cloud strokes, and can distinguish between CG strokes and IC strokes. Typical  
484 baseline of LINET systems are 200 km between adjacent sensors, allowing very good detection efficiency,  
485 even for very weak strokes (< 10 kA), whereby an average statistical location accuracy of ~200 m is  
486 achieved. However, in the HyMeX area in Southern France the baselines are longer and, thus, the  
487 efficiency is somewhat lower than in most other LINET network areas.

488

#### 489           **3.3.4 ZEUS**

490

491           The ZEUS network is a long-range lightning detection system, operated by the National  
492 Observatory of Athens. ZEUS system comprises six receivers deployed in Birmingham (UK), Roskilde  
493 (Denmark), Iasi (Romania), Larnaka (Cyprus), Athens (Greece), Lisbon (Portugal), the latter being  
494 relocated to Mazagon (Spain). ZEUS detects the impulsive radio noise emitted by a lightning strike in the  
495 Very Low Frequency (VLF) spectrum between 7 and 15 kHz. At each receiver site an identification  
496 algorithm is executed that detects a probable sferics candidate, excludes weak signal and noise and is  
497 capable of capturing up to 70 sferics per second. Then the lightning location is retrieved (at the central  
498 station) using the arrival time difference technique. Further details on ZEUS network are given in Kotroni  
499 and Lagouvardos (2008). Lagouvardos et al. (2009) have compared ZEUS system with the LINET system  
500 over a major area of Central-Western Europe where the latter system presents its major efficiency and  
501 accuracy and found that the location error of ZEUS was 6.8 km and the detection efficiency 25%. These

502 numbers are applicable also for the SOP1 domain. The authors found also that while ZEUS detects cloud-  
503 to-ground lightning it is also capable to detect strong IC lightning. At this point it should be stated that the  
504 statistical analysis showed that ZEUS is able, with high accuracy, to detect the occurrence of lightning  
505 activity although it underdetects the actual number of strokes.

506

### 507 **3.4 Instrumentation during EOP and LOP**

508

509 The only instruments operated so far during EOP and LOP are the OLLSs due to their operational  
510 design. For instance, ZEUS observations are continuously delivered in real time to HyMeX LOP web site,  
511 while EUCLID and ATDnet produce daily maps of the lightning activity over the Mediterranean Basin that  
512 are delivered to the HyMeX database. During spring 2014, a network of 12 LMA stations has been  
513 deployed permanently in Corsica to contribute to the HyMeX LOP efforts in that specific region of the  
514 Mediterranean Sea.

515

### 516 **3.5 Modeling**

517

#### 518 **3.5.1 The Meso-NH model**

519

520 The 3-D cloud-resolving mesoscale model MesoNH (see <http://mesonh.aero.obs-mip.fr>) contains  
521 CELLS, an explicit scheme to simulate the cloud electrification processes (Barthe et al., 2012). This  
522 electrical scheme was developed from a 1-moment microphysical scheme of MesoNH to compute the  
523 non-inductive charge separation rates, for which several parameterizations are available, the gravitational  
524 sedimentation of the charges and the transfer rates as the electrical charges evolve locally according to  
525 the microphysical mass transfer rates. The charges are transported by the resolved and turbulent flows.  
526 They are carried by the cloud droplets, the raindrops, the pristine ice crystals, the snow-aggregates, the  
527 graupel and the two types of positive/negative free ions to close the charge budget. The electric field is  
528 computed by inverting the Gauss equation on the model grid (vertical terrain-following coordinate). It is  
529 updated at each model time step and also after each flash when several of them are triggered in a single

530 time step. The lightning flashes are treated in a rather coarse way. They are triggered when the electric  
531 field reaches the breakeven field. A vertically propagating leader is then first initiated to connect the  
532 triggering point to the adjacent main layers of charges upwards and downwards. Then the flash  
533 propagates horizontally along the layers of charges using a fractal scheme to estimate the number of  
534 model grid points reached by the flash path. The flash extension is limited by the geometry of the charged  
535 areas and the cloud boundaries. Finally an equal amount of positive and negative charges are partially  
536 neutralized at model grid points where an IC flash goes through. In contrast, the CG flashes, detected  
537 when the height of the downward tip of the first leader goes 1500 m a.g.l., are polarized since they are not  
538 constrained by a neutralization requirement.

539

540

### 541 **3.5.2 The WRF model**

542

543 The PEACH team has already explored the use of the available observational and modeling tools  
544 for the improvement of the monitoring, understanding and forecasting of a SOP-like heavy precipitation  
545 event over Southern France (Lagouvardos et al., 2013). More specifically the authors applied in MM5  
546 mesoscale model an assimilation technique that controls the activation of the convective parameterization  
547 scheme using lightning data as a proxy for the presence of convection. The assimilation of lightning  
548 proved to have a positive impact on the representation of the precipitation field, providing also more  
549 realistic positioning of the precipitation maxima.

550 Following this example, various simulations of SOP1 case studies are expected to be performed  
551 based on WRF model. The WRF model (Skamarock et al., 2008) is a community mesoscale NWP model  
552 designed to be a flexible, state-of-the-art tool that is portable and computationally efficient on a wide  
553 variety of platforms. It is a fully compressible non-hydrostatic model with a terrain following hydrostatic  
554 pressure vertical coordinate system and Arakawa C grid staggering. It is in the authors plans to also  
555 investigate the ability of WRF model to predict the spatial and temporal distribution of lightning flashes  
556 based on the implemented scheme proposed by Barthe and Barth (2008), where the prediction of  
557 lightning flash rate is based on the fluxes of non-precipitating and precipitating ice.

558

## 559 **4-Observations collected during the HyMeX SOP1 period**

560

561 The following section presents an overview of observations collected by different PEACH  
562 instruments and demonstrates the rather comprehensive and unique dataset on natural lightning flashes  
563 collected so far in Europe. The different examples shown here are not related to any other HyMeX SOP1  
564 observations as the main goal of the paper focuses on the actual PEACH observations and their  
565 consistency. Several studies are already underway to relate the lightning activity and the electrical  
566 properties to microphysical and dynamical properties of the parent thunderclouds using observations from  
567 operational and research radars (e.g. Bousquet et al., 2014), in situ airborne and ground-based probes  
568 and satellites, and using numerical simulations.

569

### 570 **4.1 SOP1 Climatology**

571

572 Figure 2 shows a comparison of the lightning activity as sensed by Météorage over South-Eastern  
573 France for the period September-October-November (SON) during 2012 and for the period 1997--2012. It  
574 is based on the number of days with at least one lightning flash recorded per day in a regular grid of 5 km  
575 x 5 km and cumulated over the period investigated. Only flashes identified as CG flashes by Météorage  
576 algorithms are considered here. A similar climatology but for the period 1997-2011 was used to determine  
577 the most statistically electrically active area in the field domain where to deploy and operate the lightning  
578 research sensors. Although further investigations on the climatologic properties of the lightning activity are  
579 underway, Fig. 2b shows the contribution of the 2012 records on the period 1997--2012. [The year 2012](#)  
580 [was rather weak in terms of lightning activity over the center of the SOP1 domain. The electrical activity](#)  
581 [was mainly located in the far Northern part of Cévennes-Vivarais, and was more pronounced along the](#)  
582 [Riviera coastline and over the Ligurian Sea \(Fig. 2b\). About 0.3% of the 5 km x 5 km pixels of the year](#)  
583 [2012 contribute to more than 20% of the 16-year climatology. Over the 500-km side domain plotted in](#)  
584 [Fig.2a and 2b, and for a period ranging from 5 September to 6 November, the total number of days with](#)  
585 [lightning activity in 2012 reached a value of 44 days, slightly below the average value for the 16 years of](#)

586 [interest \(Fig. 2c\)](#). Even if the lightning activity was less pronounced in 2012 [over the CV domain](#), electrical  
587 properties of several convective systems were documented during SOP1 as shown in the following, in  
588 Ducrocq et al.(2013) and Bousquet et al. (2014) as well. HyLMA also captured summer thunderstorms as  
589 it was already operated before the SOP1. During the deployment of the HyLMA network, and based on  
590 the experience gained during the Deep Convective Clouds and Chemistry (DC3) project, it was decided to  
591 enhance the actual coverage of the HyLMA network by deploying four of the twelve stations  
592 (Candillargues, Mont Aigoual, Mont Perier, Mirabel) away from the dense 8-station network. The  
593 redeployment to the West was also strongly recommended by the local Weather Office to document the  
594 growth of new electrical cells within V-shape storm complexes that usually occur in the Southwestern  
595 zone of the field domain. [Interestingly, this](#) new configuration offered the possibility to record farther  
596 lightning activity in all directions.

597

## 598 **4.2 Examples of concurrent PEACH observations**

599

### 600 **4.2.1 Flash level**

601

#### 602 **4.2.1.1 A regular IC (2012/09/24 02:02:32 UT)**

603

604 Figure 3 shows an example of [a](#) regular IC flash recorded by HyLMA during SOP1 Intensive  
605 Observation Period (IOP) [IOP-06](#) on 24 September 2012. This flash was recorded within a mature  
606 convective cell. The lightning flash lasted for 800 ms. It was composed of 2510 VHF sources as  
607 reconstructed from at least 7 HyLMA stations and  $\chi^2 < 1$ . [For more information on the definition of the](#)  
608 [parameters associated to each LMA source the interested reader is referred to Thomas et al. \(2004\)](#). ,  
609 [The VHF sources were vertically](#) distributed between 4 and 12 km (Fig. 3d). The IC flash was triggered at  
610 8.5 km height (Fig. 3e). This IC flash exhibits a regular bi-level structure with long horizontal branches  
611 propagating at 6 and 11 km [asl](#) height (Fig. 3b and c). The lower branches show weaker VHF sources  
612 than the upper branches and spread over a larger altitude range (Fig. 3f). The high (low) altitude  
613 horizontal branches correspond to negative (positive) leaders propagating through positive (negative)

614 charge regions. As expected the upper channels, i.e. negative leaders, propagated faster [as evidenced](#)  
615 [from the actual distances traveled by the negative leaders compared to the ones traveled by the positive](#)  
616 [leaders during the same temporal gap](#). During the development of the flash, most of the breakdown  
617 events are detected by HyLMA at the edge of the discharges previously ionized and consequently tend to  
618 widen the lower and upper channels away from the upward channel. HyLMA partially mapped one fast  
619 process at 02:32:33.557 that lasted for 3.5 ms and propagated over 25 km from the lower part to the  
620 upper part of the flash (see the black lines in Fig. 3). [Finally, none](#) of the OLLSs reported that specific IC  
621 flash while other IC flashes have been recorded by the OLLSs.

622

#### 623 **4.2.1.2 A regular negative CG (2012/09/24 02:02:32 UT)**

624

625 Figure 4 shows a compilation of records for a negative multi-stroke CG flash as recorded by  
626 HyLMA and the different [OLLSSs, but](#) also as sampled at close range (25 km) by the [VFRS instruments](#)  
627 [and](#) one of the SLAs. The flash lasted for more than 1.1 s and was composed of 9 connections to the  
628 ground as deduced from the VFRS [Field Record](#) and video data analysis (Fig. 4e and f). HyLMA  
629 reconstructed 1464 VHF sources [derived](#) from at least 7 HyLMA stations. The VHF sources were all  
630 located below 5.5 km height (Fig. 4d) and their 3-D distribution indicates that a negative charge region  
631 was located south of the ground strokes at an average altitude of 4.5 km height (Fig. 4a--c). Note that for  
632 the present -CG flash HyLMA did not map entirely the downward stepped leaders down to the ground  
633 (Fig. 4e and f).

634 The -CG flash was recorded by all OLLSs but ZEUS (Fig. 4g). [ATDnet reported 7 events, whereas](#)  
635 [EUCLID identified 5 strokes as negative ground connections, and LINET categorized 8 strokes as](#)  
636 [negative ground connections and 1 stroke as positive ground connection](#). Times of OLLS records are  
637 obviously coincident with times of [Field Record](#) stroke records (in gray in Fig. 4e--g). The signal recorded  
638 by the SLA documented the changes induced by the successive ground connections and confirmed the  
639 negative polarity of the CG flash (Fig. 4f). The events recorded by the different OLLSs are mainly located  
640 close to each [other](#) except for one ATDnet stroke (Fig. 4a--c). Further investigations are underway to

641 study both flash and stroke detection efficiencies and location accuracy of the OLLSs over the HyLMA  
642 domain using other coincident VFRS, SLA and HyLMA records.

643 The same CG flash was also documented with the 5-ms camera as shown in Fig. 5 where the  
644 images recorded at the time of the ground [connections identified from VFRS records are](#) compiled. Times  
645 of the successive (single) frames are indicated in orange in Fig. 4g. The two first frames in Fig. 5 show  
646 clearly two channels connecting to the ground. The other frames show scattered light accompanying the  
647 successive return [strokes but with the channel itself masked by a nearby hill, except](#) the frame at  
648 01:43:18.490 where much weaker optical signal was recorded (Fig. 5). ATDnet, EUCLID and LINET  
649 detected this specific stroke (Fig. 4g) as well as the [Field Record](#) sensor (Fig. 4e), but the change induced  
650 by this stroke had little impact as detected with the SLA (Fig. 4f). The first channel to ground was recorded  
651 without any question by the video camera, but was not located by any OLLS. Interestingly a flash located  
652 42 km away from VSFR, and north to the –CG flash, triggered around the time of the first ground  
653 connection, so the radiation might have interfered with the signal radiated by the first ground connection.  
654 [Additionally, the](#) noisy [Field Record](#) signal recorded at 01:43:18.6 (Fig. 4e, elapsed time equal 1.6 s)  
655 emanated from the early stage of a 700 ms duration IC flash located 30 km north from the documented –  
656 CG flash.

657 Over the entire SOP1 campaign, several optical observations are available for other –CG flashes,  
658 for +CG flashes and also for IC flashes propagating along or below the cloud base. Even if the VFRS was  
659 mobile, it was often difficult to capture optical measurements either because of rain or presence of low-  
660 level clouds between the lightning flashes and the video camera. However the recorded [Field Record](#)  
661 observations, with and without optical measurements, of the mobile instrumentations in conjunction with  
662 SLA records offer a rather unique ground-truth to validate the OLLS records, to quantify their detection  
663 efficiency and to investigate in detail the flash processes that are recorded and located by the different  
664 OLLSs operated with short and long baselines.

665

#### 666 **4.2.1.3 Examples of unusual lightning flashes**

667

668           The more HyLMA data are being analyzed, the more we find lightning flashes that do not fit with  
669 either the bi-level structure of regular IC flashes or with the typical development of multi-stroke –CG  
670 flashes. In the following we present two examples of unusual lightning [flashes](#). For instance, [Fig. 6](#)  
671 [presents the HyLMA and OLLS records for a specific type of flash](#), called bolt-from-the-blue (BFTB) type.  
672 In the present case the flash (5 September 2012 17:51:20 UT) started like a regular IC flash with an  
673 ignition at 6 km height. Fifty milliseconds after its ignition, the upper discharge split in two parts, one  
674 progressing [continuously](#) upward, the second one going downward and propagating first at [a constant](#)  
675 [altitude of 8 km during 50 ms before descending](#) and eventually connecting to the ground. The altitude-  
676 latitude panel (Fig. 6b) shows [clearly](#) several branches of negative stepped leaders approaching the  
677 ground while the flash propagates to the ground.

678           EUCLID and LINET reported the first ground connection and a second ground strike (Fig. 6e and  
679 f). [Additionally, EUCLID and LINET reported IC events a few milliseconds after the first VHF source](#) (Fig.  
680 6g). The locations of the IC events given by EUCLID and LINET are consistent with the HyLMA [locations](#).  
681 LINET reported an IC event at an altitude of 5 km, just above the negative charge region. [This example](#)  
682 [demonstrates](#) the capability of the operational systems like EUCLID and LINET to detect IC components,  
683 and potentially IC flashes.

684           The ZEUS network did not locate any event during that specific flash. On its side ATDnet recorded  
685 the first ground connection but also the VLF radiation in the early beginning of the flash with a rather  
686 accurate location (Fig. 6a--c). This example among others confirms the capability of Sferics detecting  
687 networks to locate some IC components as Lagouvardos et al. (2009) already reported with ZEUS and  
688 LINET. The HyMeX SOP1 data offers a unique [opportunity](#) to study the CG and IC detection efficiencies  
689 as well as location accuracy, but also to investigate the discharge properties with a signal strong enough  
690 and well [pronounced](#) to be detected and located by long range VLF detection systems. Eleven BFTB  
691 flashes over a total of 124 flashes were recorded during the entire lifecycle of the 5 September 2012  
692 isolated storm with negative downward stepped leaders propagating from the upper positive charge region  
693 to the ground. Other BFTB flashes have been identified in the HyLMA dataset analyzed so far like the  
694 ones observed during the event of 24 September 2012, [the IOP-06 case](#) (not shown).

695 Figure 7 presents the example of a complex flash recorded on 30 August 2012 (04:35:00 UTC)  
696 before the beginning of SOP1. The VHF radiations were recorded over more than 5 s and the lightning  
697 flash propagated from the Northwest to the Southeast over a large domain (> 120 km long; Fig. 7a--c).  
698 [The temporal and spatial evolution of the successive discharges mapped by HyLMA reveals that the](#)  
699 [continuous VHF signal emanated from a single but extensive lightning flash](#). The flash mainly occurred on  
700 the eastern side of the HyLMA coverage area. Comparison with radar observations indicated that the flash  
701 propagated in a stratiform region (not shown). The spatial distribution of the VHF sources suggests the  
702 existence of multiple charge regions in the parent cloud at different altitudes (Fig. 7b and c). Four  
703 (seventeen) seconds before (after) the occurrence of the studied flash another long-lasting flash occurred  
704 in the same area. Flashes of 2 to 3 s duration were also recorded between 04:00 UTC and 05:00 UTC  
705 mostly in the northwestern part of the storm complex. Forty-four flashes were recorded between 04:30  
706 UTC and 04:40 UTC over the domain of interest, all but the one shown in Fig. 7 occurring in the  
707 northwestern electrical cell centered at 44.5°N and 5°E.

708 All OLLSs reported space and time consistent observations relatively to HyLMA records. ATDnet  
709 reported 4 fixes, EUCLID 14 events including 8 negative ground strokes and 1 positive ground stroke,  
710 LINET 14 [events, all identified as ground strokes as no altitude information was available, and](#) ZEUS 7  
711 fixes. A single flash identified by HyLMA is actually seen as multiple flashes by the OLLSs with the  
712 algorithms used to combine strokes/fixes [into](#) flashes. This unusual flash [example demonstrates](#) the  
713 relevance and the usefulness of VHF mapping to characterize the full 3-D spatial extension of the lightning  
714 flashes. [Additionally, some of the events detected by one OLLS are also detected by one or more](#)  
715 [other OLLSs, while sometimes some events are reported by one single OLLS only](#). This was also  
716 observed during the analysis of the lightning data for the 6--8 September 2010 storm but not discussed in  
717 Lagouvardos et al. (2013). Such discrepancy is explained by the differences between the four OLLSs in  
718 terms of technology, range and amplitude sensibility, detection efficiency and location algorithms. For the  
719 studied flash, coincident OLLS strokes are observed with a time difference from 60 to 130  $\mu$ s between  
720 long range and short range OLLSs and around 20  $\mu$ s between EUCLID and LINET.

721

#### 722 **4.2.1.4 Concurrent VHF and acoustic measurements**

723  
724 Acoustic and infrasonic measurements were performed during HyMeX SOP1 as detailed in Sect.  
725 3.2.3. Figure 8 presents an example of concurrent records during 2.5 min of the lightning activity sensed  
726 on 24 September 2012. During that period, HyLMA detected seven lightning flashes (with one composed  
727 of a few VHF sources) in the studied area (Fig. 8a and e), all inducing a moderate to significant change on  
728 the SLA signal (Fig. 8g). ATDnet sensed all flashes except the one composed of a few VHF sources at  $T$   
729 = 48 s (Fig. 8g). EUCLID, LINET and ZEUS recorded all but two flashes including the one composed of a  
730 few VHF sources, the second flash being not the same for these three OLLSs. ZEUS erroneously located  
731 additional flashes in the domain of interest. Among the seven flashes, three were connected to the ground  
732 with a negative polarity (Fig. 8g). The lightning activity was located about 20 km away from the acoustic  
733 sensors marked with a red diamond in Fig. 8a. The time evolution of the pressure difference (Fig. 8e)  
734 traces two acoustic events of duration greater than 20 s. The first event, between  $T=40$  s and  $T=70$  s is  
735 related to the first IC flash recorded during the first seconds of the studied period. The second acoustic  
736 event, starting at  $T=105$  s, comes from the two flashes (one –CG and one IC) recorded between  $T=60$  s  
737 and  $T = 70$  s. The propagation of sound waves in the atmosphere and the properties of the atmosphere  
738 along the acoustic path to the acoustic sensors are at the origin of the delay between the recording of the  
739 electromagnetic signal and the recording of the acoustic signal. For the first acoustic event, the acoustic  
740 spectrogram (Fig. 8f) reveals a series of three acoustic bursts while for the second acoustic event, the  
741 spectrogram shows a lesser powerful signal. A signal of 0.2 Pa (absolute value) received by the sensors  
742 20 km away from the storm is in the amplitude range of acoustical signals usually recorded. Based on the  
743 unique dataset collected during the SOP1, several studies have been performed to relate the acoustic  
744 signal and its spectral and temporal properties to the original lightning flash type and properties.

745

#### 746 4.2.2 Examples of SOP1 daily lightning activity as recorded by HyLMA

747

748 The previous sections showed a series of concurrent records at the flash scale. Here we discuss  
749 on some storms recorded during the SOP1 period. Note that lightning activity recorded during the June--  
750 August period is not discussed here but it is worth to mention that different types of storms were fully

751 recorded during the entire HyLMA operation. As an example, Fig. 9 shows daily lightning maps as  
752 produced only from HyLMA data with, for each considered day the 10-min VHF source rate reconstructed  
753 from at least 7 LMA stations over the HyLMA coverage area in panel (a), the geographical distribution of  
754 the lightning activity (the grayscale is time related) with an overlay of the 1-h VHF source density (per  
755  $0.025^{\circ} \times 0.025^{\circ}$ ) at one specific hour in panel (b), and the vertical distribution of the VHF sources (per  
756  $0.025^{\circ} \times 200\text{m}$ ) computed during the hour indicated at the top of the figure in panel (c). As already  
757 mentioned, different types of convective systems were recorded during the operation of HyLMA ranging  
758 from gentle isolated thunderstorms to organized and highly electrical convective lines between June 2012  
759 and November 2012.

760 Figure 9A shows the lightning activity recorded during the IOP-01 (11 September 2012) with  
761 scattered deep convection developing in early afternoon (Fig. 9A.a) over Southeastern Massif Central,  
762 and due to a convergence between a slow southeasterly flow from the Mediterranean Sea and a westerly  
763 flow from the Atlantic. The convection remained isolated and mainly confined to mountainous areas, with  
764 some cells reaching the foothills in late afternoon due to the westerly mid-level flow (Fig. 9A.b). The  
765 French F20 research aircraft, with the airborne 95 GHz Doppler cloud radar named RASTA (RADar  
766 SysTem Airborne) and in situ microphysics probes, sampled the anvils of the closest convective cells to  
767 the HyLMA stations. The rainfall accumulation ranged from 5 to 10 mm in 24h, and reached locally levels  
768 of up to 30-40 mm in Ardèche. This example shows typical observations collected with HyLMA during  
769 scattered convection over the domain of interest, definitively demonstrating that the records of HyLMA as  
770 well as the records of OLLSs offer the possibility of a radar-like tracking of storm motions.

771 Figure 9B shows the HyLMA records during the IOP-06 (24 September 2012). An intense and fast  
772 moving convective line crossed the CV domain during the early morning, Liguria--Tuscany by mid-day and  
773 Northeastern Italy in the evening with an amount of rainfall observed of 100mm/24hr over South-Eastern  
774 France, with rainfall intensity up to 50-60 mm/hr and wind gusts up to 90-100km/h locally. The storm  
775 activity started in the evening of 23 September on the west side of the HyLMA network and moved to the  
776 east with successive electrical cells developing and merging. Figure 9B.b and c show one of the highest  
777 density of VHF sources recorded during the entire period of HyLMA operation. Between 02:00 UTC and  
778 03:00 UTC, the lightning activity was more or less distributed along a north-south direction but then

779 extended further north to the HyLMA network (Fig. 9B.b). Focusing on the electrical cells located in the  
780 vicinity of the LMA network, the lightning activity was located at the east of strong updrafts retrieved from  
781 the radar data (see Fig. 8 in Bousquet et al., 2014) with the deepest electrified convective cell reaching up  
782 to 13 km height. Many different PEACH instruments documented the lightning activity of this storm as  
783 shown in Figs. 3, 4 and 8. The VFRS was operated from the Aubenas airfield (44.538°N, 4.371°E) from  
784 the early hours of the storm activity to mid-morning. Some storm cells were also documented with the  
785 airborne RASTA radar and in situ microphysics probes on board the F20, and by different precipitation  
786 research radars located in the Northern part of the HyLMA coverage area.

787 Figure 9C shows the total lightning activity sensed during the IOP-07a (26 September 2012). A  
788 first convective system appears early in the morning over the HyLMA because of a warm, unstable and  
789 convergent air mass that merges with a frontal system progressing eastwards during the afternoon. This  
790 event brings more than 100 mm in 24h over the Cévennes-Vivarais region. Additionally the city of Nice on  
791 the Riviera Coast was flooded in the evening (Fig. 9C.b). The VFRS was operated from Valence  
792 (44.992°N 4.887°E) during the first part of the day, and then at Mont Ventoux (44.171°N, 5.202°E). During  
793 the morning observations, most CG flashes recorded with VFRS instruments in the northern part of the  
794 convective complex were of positive polarity, while the CG flashes in the afternoon were mostly negative.

795 Figure 9D shows the HyLMA records for the 29 September 2012 (IOP-08). This system moved  
796 from Spain where heavy precipitation was recorded on the north-easterly flank of Spain with casualties  
797 and significant damages. Figure 9D.b shows a rather well coverage by the HyLMA in its southeastern  
798 sector with more pronounced altitude errors for very distant flashes. The case is interesting as it moved  
799 from sea to land (Fig. 9D.b) and should allow to investigate contrasting lightning properties over sea and  
800 over land but also to document the transition from sea to land. VFRS observations were collected for  
801 lightning flashes along the Riviera.

802 Figure 9E shows the lightning activity of IOP-13 (14 October 2012) where Nice airport was closed  
803 at the end of the day because of strong vertical shear. A tornado (EF1) was observed in the vicinity of  
804 Marseille between 14:00 UTC and 15:00 UTC. The analysis of the lightning activity of the tornado cloud  
805 revealed the occurrence of a convective surge with a sudden increase of the flash rate and an upward  
806 shift of the flash triggering altitude (not shown). Analysis combining HyLMA, OLLSs, and operational

807 radar records is underway to evaluate the benefit of lightning detection in terms of information precursor  
808 related to this tornado. [Additionally, the](#) French F20 aircraft sampled some electrified clouds but later  
809 (17:00--20:00 UTC) to perform a survey of precipitating systems over Provence/Côte d'Azur (French  
810 Riviera), [which offers](#) the possibility to study in situ microphysics, vertical structure of the clouds and  
811 lightning activity.

812 [Finally](#), Fig. 9F shows the observed lightning activity during [IOP-16a](#) (26 October 2012). A first  
813 system affected the Hérault and Gard departments in the morning but a second more intense system  
814 developed in the southeast of France in the afternoon with two casualties in Toulon. Rain accumulation  
815 reached up to 170 mm in 24 h on the CV domain. The F20 aircraft flew between 06:00 UTC and 09:30  
816 UTC in the complex located [at](#) 43°N, 4°E (Fig. 9F.b). A second F20 flight sampled the electrically active  
817 storms shown in Fig. 9F.b (43.2°N, 6°E; 43.2°N, 3°E). VFRS observations were performed at the end of  
818 the day about 50-km east of the HyLMA network for a series of mainly -CG flashes. Between 20:30 UTC  
819 and 20:40 UTC the lightning activity sensed in the vicinity of the MBA/MPA network was rather weak (i.e.  
820 24 flashes in 10 min) so one-to-one correlations between RF HyLMA and EUCLID records and non-noisy  
821 acoustics signals from [the](#) same flashes are currently being studied (not shown).

822

## 823 **5-Prospects**

824

825 The present article summarizes only a small number of observed events made with the different  
826 PEACH instruments during HyMeX SOP1. This rather unique and comprehensive lightning dataset  
827 collected during the SOP1 period will serve to investigate the properties of individual lightning flashes but  
828 also to probe objectively, for the first time, the performances of European OLLSs in the Southeastern  
829 France and close to the Mediterranean Sea. This task will help [to](#) refine our current knowledge on what  
830 European OLLSs actually record and more specifically which intra-cloud processes are detected and  
831 located. The investigation should eventually provide new insights on the potential of IC detection from  
832 European OLLSs for operational storm tracking and monitoring over the entire Mediterranean Basin.

833 Several analyses are already underway to investigate the properties of the lightning activity from  
834 the flash scale to the regional scale in relation with cloud and atmospheric properties as derived from

835 satellite imagery, operational/research ground-based and airborne radars, rain gauges and in situ  
836 microphysical probes. The analyses focuses not only on HyMeX SOP1 priority cases (Ducrocq et al.,  
837 2013) but also on non-SOP1 events as HyLMA data cover from June 2012 to end of November 2012. The  
838 analysis will eventually provide key lightning-related indexes to describe the electrical nature of  
839 thunderstorms in Southeastern France and [which will be used](#) in multi-disciplinary studies carried out  
840 within HyMeX. The combination of HyLMA and OLLS records will provide a set of basic products, e.g.  
841 flash rate, flash type, flash properties, flash density to feed the HyMeX database.

842 The HyMeX case studies are not only observationally-oriented but are also intended to provide  
843 material for verification and validation of km-scale electrified cloud simulations (e.g. Pinty et al., 2013).  
844 Indeed successful simulations are already performed and comparisons of simulated and observed  
845 parameters, [e.g. vertical distribution of the charge regions, flash location, flash rate, flash extension](#), are  
846 already showing promising results. The HyLMA data should then help [to](#) identify objectively which non-  
847 inductive charging process treatment (“Takahashi” versus “Saunders”) leads to the best simulation results.

848 An objective debriefing of SOP1 preparation, operation and data analysis will be performed [in the](#)  
849 [near future](#) to identify the successes and the failures. This is to help us to refine the preparation of a  
850 dedicated Atmospheric Electricity field campaign in early autumn 2015 over the Corsica Island as a  
851 permanent LMA [was settled there in May 2014](#) for [a minimum of](#) five years at least. Another region of  
852 interest is the Eastern Mediterranean Sea during fall where an electrical activity takes place over the sea  
853 but ceases when the thunderclouds are landing.

854 [Finally, the](#) different activities performed around the PEACH project already helped us gain  
855 expertise not only for field deployment and operations but also in terms of data analysis methodologies,  
856 realistic lightning and cloud simulations and application of lightning detection for very short range forecast  
857 in preparation for the EUMETSAT Meteosat Third Generation Lightning Imager (launch scheduled early  
858 2019).

859

859 **Acknowledgements**

860 This project was sponsored by Grants MISTRALS/HyMeX and ANR-11-BS56-0005 IODA-MED. LEFE-  
861 IDAO, Université de Toulouse, the GOES-R Visiting program also supported the PEACH project during  
862 its preparation and the field campaign. The Greek contribution to PEACH objectives is partially funded by  
863 the TALOS project funded in the frame of “ARISTEIA II” by the Greek General Secretariat for Research  
864 and Technology. We are grateful to R. Blakeslee and NASA for lending the MSFC LMA during the SOP1  
865 period. We would like to thank the team of local Météo-France weather office in Nîmes for its strong  
866 support during the site survey, the deployment, the operation and the dismantlement of the instruments,  
867 and for letting us deployed four of the HyLMA stations on Météo-France lands. We also thank Mr. and Ms.  
868 Imbert (Cadignac HyLMA site), Mr. Rey and the Méjannes Le Clap City Council (Méjannes Le Clap  
869 HyLMA site), Mr. Comte (Vic Le Fesq HyLMA site), Mr. and Ms. Bazalgette (Mont Aigoual HyLMA site),  
870 Mr. Vincent (Mont Perier HyLMA site), Mr. Chaussedent (Mirabel HyLMA site), Mr. Fourdrigniez (CCI Alès  
871 Deaux airfield HyLMA site) and Mr. Garrouste (CNRM-GAME, responsible of the Candillargues HyMeX  
872 Supersite; Candillargues HyLMA site) who hosted a HyLMA station. We also thank Mr. Reboulet (Mayor  
873 of La Bruguière) for allowing the deployment of one SLA and the MBA/MPA package on his property. We  
874 also thank Mr. Cerpedes (Grand Combe Technical Manager) for letting us to deploy the second SLA on  
875 Grand Combe airfield. We are also grateful to the different weather forecasters and the HyMeX Operation  
876 Direction for the support to the VFRS. We thank Georg Pistotnik from the European Severe Storm  
877 Laboratory (ESSL) for providing additional special forecasts in preparation and during several VFRS  
878 observation trips. We also thank Brice Boudevilain (LTHE) and Olivier Bousquet (Météo-France) for  
879 providing contacts for the deployment of the four most remote HyLMA stations.

880

880 **References**

- 881 Adamo, C. (2004), On the use of lightning measurements for the microphysical analysis and  
882 characterization of intense precipitation events over the Mediterranean area, Ph.D. dissertation, Univ.  
883 of Ferrara, Ferrara, Italy.
- 884 Altaratz, O., T. Reisin and Z. Levin (2005), Simulation of the Electrification of Winter Thunderclouds using  
885 the 3-dimensional RAMS Model: single cloud simulations. *J. Geophys. Res.*, 110, D20205, 1-12.
- 886 Arechiga, R. O., J. B. Johnson, H. E. Edens, R. J. Thomas, and W. Rison (2011), Acoustic localization of  
887 triggered lightning, *J. Geophys. Res.*, 116, D09103, doi:10.1029/2010JD015248.
- 888 Barthe, C., M. Chong, J.-P. Pinty, C. Bovalo, and J. Escobar (2012), Updated and parallelized version of  
889 an electrical scheme to simulate multiple electrified clouds and flashes over large domains, *Geosci.*  
890 *Model Dev.*, 5, 167-184, doi:10.5194/gmd-5-167-2012.
- 891 Barthe C., and M. C. Barth (2008), Evaluation of a new lightning-produced NO<sub>x</sub> parameterization for cloud  
892 resolving models and its associated uncertainties, *Atmos. Chem. Phys.*, 8, 4691–4710.
- 893 Barthe C., J.-P. Pinty (2007a), Simulation of electrified storms with comparison of the charge structure and  
894 lightning efficiency, *J. Geophys. Res.*, 112, D19204, doi:10.1029/2006JD008241.
- 895 Barthe C., J.-P. Pinty (2007b), Simulation of a supercellular storm using a three-dimensional mesoscale  
896 model with an explicit lightning flash scheme, *J. Geophys. Res.*, 112, D06210,  
897 doi:10.1029/2006JD007484.
- 898 Barthe C., J.-P. Pinty, C. Mari (2007c), Lightning-produced NO<sub>x</sub> in an explicit electrical scheme tested in a  
899 Stratosphere-Troposphere Experiment: Radiation, Aerosols, and Ozone case study, *J. Geophys. Res.*,  
900 112, D04302, doi:10.1029/2006JD007402.
- 901 Barthe, C., G. Molinié and J.-P. Pinty (2005), Description and first results of an explicit electrical scheme  
902 in a 3D cloud resolving model, *Atmos. Res.*, 76, 95–113.
- 903 [Beard, K. V., Terminal velocity and shape of cloud and precipitation drops aloft, \*J. Atmos. Sci.\*, 33, 851–](#)  
904 [864, 1976.](#)
- 905 Betz, H.-D., K. Schmidt, and W. P. Oettinger (2008), LINET - An International VLF/LF Lightning Detection  
906 Network in Europe, in "Lightning: Principles, Instruments and Applications", Eds. H.-D.. Betz, U.  
907 Schumann, and P. Laroche, ch. 5, Dordrecht (NL), Springer.

908 Betz, H.-D., K. Schmidt, P. Laroche, P. Blanchet, W. P. Oettinger, E. Defer, Z. Dziewit, and J. Konarski  
909 (2009), LINET - an international lightning detection network in Europe, *Atmos. Res.*, 91, 564–573.

910 ~~Blanc, E., A. Le Pichon, L. Ceranna, T. Farges, J. Marty, and P. Herry (2010), Global scale monitoring of~~  
911 ~~acoustic and gravity waves for the study of the atmospheric dynamics, in *Infrasound Monitoring for*~~  
912 ~~*Atmospheric Studies*, edited by A. Le Pichon, E. Blanc, and A. Hauchecorne, pp. 647–664,~~  
913 ~~doi:10.1007/978-1-4020-9508-5\_21, Springer, Dordrecht, Netherlands.~~

914 Blanc, E., T. Farges, A. Le Pichon, and P. Heinrich (2014), Ten year observations of gravity waves from  
915 thunderstorms in western Africa, *J. Geophys. Res. Atmos.*, 119, doi:10.1002/2013JD020499.

916 Bousquet, O., et al. (2014), Multiple-Frequency Radar Observations Collected In Southern France During  
917 The Field Phase Of The Hydrometeorological Cycle In The Mediterranean Experiment (HyMeX),  
918 BAMS, in revision.

919 Chauzy, S. and S. Soula, 1987, General interpretation of surface electric field variations between lightning  
920 flashes, *J. Geophys. Res.*, 92(D5), 5676-5684.

921 Christian, H. J., and Coauthors (2003), Global frequency and distribution of lighting as observed from  
922 space by the Optical Transient Detector. *J. Geophys. Res.*, 108, D14005, doi:10.1029/2003JD002347.

923 Coquillat, S., B. Combal, and S. Chauzy (2003), Corona emission from raindrops in strong electric fields  
924 as a possible discharge initiation: comparison between horizontal and vertical field configurations, *J.*  
925 *Geophys. Res.* 108 (D7), 4205, doi:10.1029/2002JD002714.

926 Coquillat, S., and S. Chauzy (1994), Computed conditions of corona emission from raindrops, Corona  
927 emission from raindrops in strong electric fields as a possible discharge initiation: comparison between  
928 horizontal and vertical field configurations, *J. Geophys. Res.* 99 (D8), 16897-16905.

929 Crabb, J. A., and J. Latham (1974), Corona from colliding drops as a possible mechanism for the  
930 triggering of lightning, *Q. J. R. Meteorol. Soc.* 100, 191–202.

931 Cummins, K., M. Murphy, E. Bardo, W. Hiscox, R. Pyle, and A. Pifer (1998), A Combined TOA-MDF  
932 Technology Upgrade of the U.S. National Lightning Detection Network, *J. Geophys. Res.*, 103(D8),  
933 9035-9044.

934 Defer, E., and P. Laroche (2008), Observation and Interpretation of Lightning Flashes with  
935 Electromagnetic Lightning Mapper, in "Lightning: Principles, Instruments and Applications", Eds. H.-D..  
936 Betz, U. Schumann, and P. Laroche, ch. 5, Dordrecht (NL), Springer..

937 Defer, E., K. Lagouvardos, and V. Kotroni (2005), Lightning activity in Europe as sensed by long range  
938 NOA-ZEUS and UK Met Office ATD VLF lightning systems and NASA TRMM-LIS sensor, Geophysical  
939 Research Abstracts, Vol. 7, 03026.

940 Defer, E., P. Blanchet, C. Théry, P. Laroche, J. Dye, M. Venticinque, and K. Cummins (2001), Lightning  
941 activity for the July 10, 1996, storm during the Stratosphere-Troposphere Experiment: Radiation,  
942 Aerosol, and Ozone-A (STERAO-A) experiment, J. Geophys. Res., 106, 10,151-10,172.

943 Ducrocq, V., et al. (2013), HyMeX-SOP1, the field campaign dedicated to heavy precipitation and flash  
944 flooding in the northwestern Mediterranean, BAMS, 10.1175/BAMS-D-12-00244.1, in press.

945 Duffourg, F. and V. Ducrocq (2011), Origin of the moisture feeding the Heavy Precipitating Systems over  
946 Southeastern France. Natural Hazards and Earth System Science, 11, 4, 1163-1178.

947 Farges, T., and E. Blanc (2010), Characteristics of infrasound from lightning and sprites near  
948 thunderstorm areas, J. Geophys. Res., 115, A00E31, doi:10.1029/2009JA014700.

949 Füllekrug M., I. Kolmasova, O. Santolik, T. Farges, J. Bor, A. Bennett, M. Parrot, W. Rison, F. Zanotti, E.  
950 Arnone, A. Mezentsev, R. Lan, L. Uhler, G. Harrison, S. Soula, O. van der Velde, J-L Pinçon, C. Helling,  
951 D. and Diver (2013), Electron Acceleration Above Thunderclouds, Environ. Res. Lett., 8, 035027,  
952 doi:10.1088/1748-9326/8/3/035027.

953 Funatsu, B., C. Claud, and J.-P. Chaboureau (2009), Comparison between the Large-Scale Environments  
954 of Moderate and Intense Precipitating Systems in the Mediterranean Region. Mon. Wea. Rev., 137,  
955 3933-3959.

956 Gaffard, C., J. Nash, N. Atkinson, A. Bennett, G. Callaghan, E. Hibbett, P. Taylor, M. Turp, and W. Schulz  
957 (2008), Observing lightning around the globe from the surface, in: the Preprints, 20th International  
958 Lightning Detection Conference, Tucson, Arizona, pp. 21–23.

959 [Gallin, L.-J. \(2014\), Caractérisation acoustique des éclairs d'orage, Ph.D. dissertation, Université Pierre et](#)  
960 [Marie Curie, Paris, France.](#)

961 Goodman, S.J., D.E. Buechler, P.D. Wright, and W. D. Rust (1988), Lightning and precipitation history of a  
962 microburst-producing storm. *Geophys. Res. Lett.* 15, 1185-1188.

963 Gurevich A. V., G. M. Milikh and G. M. Roussel-Dupre (1992), Runaway electron mechanism of air  
964 breakdown and preconditioning during a thunderstorm, *Phys. Letter, A* (165), 463-468.

965 Helsdon J. H. Jr., S. Gattaleeradapan, R. D. Farley, and C. C. Waits, 2002, An examination of the  
966 convective charging hypothesis: Charge structure, electric fields, and Maxwell currents, *J. Geophys.*  
967 *Res.*, 107 (D22), 4630, doi:10.1029/2001JD001495.

968 Helsdon, J., Jr., and R. Farley, 1987, A Numerical Modeling Study of a Montana Thunderstorm: 2. Model  
969 Results Versus Observations Involving Electrical Aspects, *J. Geophys. Res.*, 92(D5), 5661-5675.

970 Holt, M. A., P. J. Hardaker, and G. P. McLelland (2001), A lightning climatology for Europe and the UK,  
971 1990 – 99, *Weather*, 56, 290 – 296.

972 Jacobson A.R , S. O. Knox, R. Franzand and D. C. Enemark (1999), FORTE observations of lightning  
973 radio-frequency signatures: Capabilities and basic results, *Radio Sci.*, 34 (2), 337-354.

974 Kohn M., E. Galanti, C. Price, K. Lagouvardos and V. Kotroni (2011), Now-Casting Thunderstorms in the  
975 Mediterranean Region using Lightning Data. *Atmospheric Research*, 100, 489-502.

976 Kotroni V and K. Lagouvardos (2008), Lightning occurrence in relation with elevation, terrain slope and  
977 vegetation cover in the Mediterranean, *J Geophys. Res*, 113, D21118, doi:10.1029/2008JD010605.

978 Krehbiel, P. R., R. J. Thomas, W. Rison, T. Hamlin, J. Harlin, and M. Davis (2000), GPS-based mapping  
979 system reveals lightning inside storms, *EOS*, 81, 21-25.

980 Kummerow, C., W. Barnes, T. Kozu, J. Shiue, and J. Simpson (1998), The tropical rainfall measuring  
981 mission (TRMM) sensor package, *J. Atmos. Oceanic Technol.*, 15, 809–817.

982 Lagouvardos, K., V. Kotroni, E. Defer and O. Bousquet (2013), Study of a heavy precipitation event over  
983 southern France, in the frame of HYMEX project: Observational analysis and model results using  
984 assimilation of lightning. *Atmospheric Research*, Volume 134, Pages 45-55.

985 Lagouvardos, K., V. Kotroni, H.-D. Betz, and K. Schmidt (2009), A comparison of lightning data provided  
986 by ZEUS and LINET networks over Western Europe, *Nat. Hazards Earth Syst. Sci.*, 9, 1713–1717.

987 Light, T. E., and co-authors (2001), Coincident Radio Frequency and Optical Emissions from Lightning,  
988 Observed with the FORTE Satellite, *J. Geophys. Res.*, 106, p. 28223-28231.

989 [MacGorman, D. R., and W. D. Rust, The electrical nature of storms, Oxford University Press, New York,](#)  
990 [pp 422, 1998.](#)

991 MacGorman, D. R., A. A. Few, and T. L. Teer (1981), Layered lightning activity, *J. Geophys. Res.*, 86,  
992 9900–9910, doi:10.1029/JC086iC10p09900.

993 [Mäkelä, A., T. J. Tuomi, and J. Haapalainen \(2010\), A decade of high-latitude lightning location: Effects of](#)  
994 [the evolving location network in Finland, J. Geophys. Res., 115, D21124, doi:10.1029/2009JD012183.](#)

995 Mansell E. R., D. R. MacGorman, C. L. Ziegler, and J. M. Straka (2002), Simulated three-dimensional  
996 branched lightning in a numerical thunderstorm model, *J. Geophys. Res.*, 107 (D9), 4075,  
997 doi:10.1029/2000JD000244.

998 Marshall T. C., M. Stolzenburg, C. R. Maggio, L. M. Coleman, P. R. Krehbiel, T. Hamlin, R. J. Thomas,  
999 and W. Rison (2005), Observed electric fields associated with lightning initiation, *Geophys. Res. Lett.*,  
1000 32, L03813, doi:10.1029/2004GL021802

1001 MacGorman D.R., D.W. Burgess, V. Mazur, W.D. Rust, W. L. Taylor and B. C. Johnson (1989), Lightning  
1002 rates relative to tornadic storm evolution on 22 May 1981, *J. of the Atmos. Sci.*, 46, 221-250.

1003 Molinié, G., J.-P. Pinty and F. Roux (2002), Some explicit microphysical and electrical aspects of a Cloud  
1004 Resolving Model: Description and thunderstorm case study, *C. R. Physique*, 3, 1- 20.

1005 Montanyà, J., Soula, S., Murphy, M., March, V., Aranguren, D., Solà, G., Romero D. (2009). Estimation of  
1006 charge neutralized by negative cloud-to-ground flashes in Catalonia thunderstorms. *J of Electrostatics*,  
1007 67, Issues 2-3, May 2009, Pages 513-517.

1008 Montanyà, J., S. Soula, N. Pineda (2007), A study of the total lightning activity in two hailstorms, *J.*  
1009 *Geophys. Res.*, 112, D13118, doi:10.1029/2006JD007203.

1010 [Orville, R. E., G. R. Huffines, W. R. Burrows, and K. L. Cummins \(2011\), The North American Lightning](#)  
1011 [Detection Network \(NALDN\)—Analysis of Flash Data: 2001–09. \*Mon. Wea. Rev.\*, 139, 1305–1322.](#)

1012 Pinty, J.-P., C. Barthe, E. Defer, E. Richard, and M. Chong (2013), Explicit simulation of electrified clouds:  
1013 from idealized to real case studies, *Atmos. Res.*, 123, 82-92.

1014 Poeppel, K. (2005), A 3D Lightning parameterization with branching and charge induction, Master's  
1015 thesis, S. D. Sch. of Mines and Technol., Rapid City.

1016 Proctor, D. E. (1981), VHF radio pictures of cloud flashes, *J. Geophys. Res.*, 86, 4041-4071.

1017 Price C., Y. Yair, A. Mugnai, K. Lagouvardos, M. C. Llasat, S. Michaelides, U. Dayan, S. Dietrich, F. Di  
1018 Paola, E. Galanti, L. Garrote, N. Harats, D. Katsanos, M. Kohn, V. Kotroni, M. Llasat-Botija, B. Lynn, L.  
1019 Mediero, E. Morin , K. Nicolaidis, S. Rozalis, K. Savvidou, and B. Ziv (2011), Using lightning data to  
1020 better understand and predict flash floods in the Mediterranean. *Surveys in Geophysics* 32 (6) , pp.  
1021 733-751.

1022 Rison, W., R.J. Thomas, P.R. Krehbiel, T. Hamlin, and J. Harlin (1999), A GPS-based Three-Dimensional  
1023 Lightning Mapping System: Initial Observations in Central New Mexico, *Geophysical Research Letters*,  
1024 26, 3573-3576.

1025 Rust, W. D., D. R. MacGorman, E. C. Bruning, S. A. Weiss, P. R. Krehbiel, R. J. Thomas, W. Rison, T.  
1026 Hamlin and J. Harlin (2005), Inverted-polarity electrical structures in thunderstorms in the Severe  
1027 Thunderstorm Electrification and Precipitation Study (STEPS), *Atmospheric Research*, 76, 247-271.

1028 Saunders, C. P. R., W. D. Keith and P. P. Mitzeva (1991), The effect of liquid water on thunderstorm  
1029 charging, *J. Geophys. Res.*, 96, 11007-11017.

1030 Saunders CPR. (2008), Charge separation mechanisms in clouds, *Space Sci. Rev.*, 137, 335-353.

1031 Schroeder, V., M. B. Baker and J. Latham (1999), A model study of corona emission from hydrometeors,  
1032 *Quaterly J. Roy. Met. Soc.*, 125, 1681-1693.

1033 Schulz, W., B. Lackenbauer, H. Pichler, and G. Diendorfer (2005), LLS Data and Correlated Continuous  
1034 E-Field Measurements, VIII International Symposium on Lightning Protection (SIPDA), Sao Paulo,  
1035 Brazil.

1036 Schulz, W., and M. M. F. Saba (2009), First Results of Correlated Lightning Video Images and Electric  
1037 Field Measurements in Austria, X International Symposium on Lightning Protection (SIPDA), Curitiba,  
1038 Brazil, November.

1039 [Schulz, W., D. Poelman, S. Pedeboy, C. Vergeiner, H. Pichler, G. Diendorfer, and S. Pack \(2014\),](#)  
1040 [Performance validation of the European Lightning Location System EUCLID, International Colloquium](#)  
1041 [on Lightning and Power Systems \(CIGRE\), Lyon, France.](#)

1042 Schultz, C., W. A. Petersen, and L. D. Carey (2011), Lightning and Severe Weather: A Comparison  
1043 between Total and Cloud-to-Ground Lightning Trends, *Weather and Forecasting*, 26, 744-755,  
1044 10.1175/WAF-D-10-05026.1.

1045 Shao X.-M., and P. R. Krehbiel (1996), The spatial and temporal development of intracloud lightning, J.  
1046 Geophys. Res., 101, 26,641-26,668.

1047 Skamarock, W. C., Klemp, J. B., Dudhia, J., Gill, D., Barker, M., Duda, X-Y. Huang, W. Wang, and J. G.  
1048 Powers (2008), A description of the Advanced Research WRF version 3. NCAR Tech. Note NCAR/TN-  
1049 475+ STR, 113 pp.

1050 Smith D. A., K. B. Eack, J. Harlin, M. J. Heavner, A. R. Jacobson, R. S. Massey, X. M. Shao, and K. C.  
1051 Wiens (2002), The Los Alamos Sferic Array: A research tool for lightning investigations, J. Geophys.  
1052 Res., 107 (D13), 4183, doi:10.1029/2001JD000502.

1053 Stephens, G. L., and Coauthors (2002), The Cloudsat mission and the A-Train, *Bull. Amer. Meteor. Soc.*,  
1054 83, 1771–1790, doi: <http://dx.doi.org/10.1175/BAMS-83-12-1771>

1055 Stolzenburg, M., W. D. Rust, and T. C. Marshall (1998), Electrical structure in thunderstorm convective  
1056 regions. 3. Synthesis, J. Geophys. Res., D103, 14,097-14,108.

1057 Soula, S., S. Chauzy, M. Chong, S. Coquillat, J.F. Georgis, Y. Seity, and P. Tabary (2003), Surface  
1058 precipitation current produced by convective rains during MAP, J. Geophys. Res., 108(D13), 4395,  
1059 doi:10.1029/2001JD001588.

1060 Soula, S. and J.F. Georgis (2013), Surface electrical field evolution below the stratiform region of MCS  
1061 storms, Atmos. Res., 132–133, pp 264-277.

1062 Standler, R. B., and W. P. Winn (1979), Effects of coronae on electric fields beneath thunderstorms, Q. J.  
1063 R. Meteorol. Soc., 105(443), 285-302.

1064 Takahashi, T. (1978), Riming electrification as a charge generation mechanism in thunderstrom, J. Atmos.  
1065 Sci., 35, 1536-1548.

1066 Thomas, R.J., P.R. Krehbiel, W. Rison, S.J. Hunyady, W.P. Winn, T. Hamlin, and J. Harlin (2004),  
1067 Accuracy of the Lightning Mapping Array J. Geophys. Res., 109, 34 pp., D14207,  
1068 doi:10.1029/2004JD004549.

1069 Yair, Y., B. Lynn, C. Price, V. Kotroni, K. Lagouvardos, E. Morin, A. Mugnai and M. C. Llasat (2010),  
1070 Predicting the potential for lightning activity in Mediterranean storms based on the Weather Research  
1071 and Forecasting (WRF) model dynamic and microphysical fields. JGR-Atmospheres, 115, D04205,  
1072 doi:10.1029/2008JD010868.

1073 Williams, E., B. Boldi,, A. Matlin, M. Weber, S. Hodanish, D. Sharp, S. Goodman, R. Raghavan, and D.  
1074 Buechler (1999), The behavior of total lightning activity in severe Florida thunderstorms. Atmos. Res.,  
1075 51, 245-265.

1076 Ziegler C.L., D.R. MacGorman, J.E. and P.S. Ray (1991), A model evaluation of noninductive graupel-ice  
1077 charging in the early electrification of a mountain thunderstorm, J. Geophys. Res., 96, 12833-12855.  
1078

1078

ID #	Location	Type	Owner	Instruments				
				LMA	SLA	MBA/ MPA	INR	EFM
1	Alès	Building roof	EMA school				X	X
2	Cadignac	Land	Private	X				
3	Candillargues	Airfield	Local administration	X			X	X
4	Deaux	Airfield	Local administration	X				
5	Grand Combe	Airfield	MF / Local administration	X	X			
6	Lavilledieu	Building roof	Elementary school				X	X
7	Méjannes Le Clap	Land	Local administration	X				
8	Mirabel	Land	Private	X				
9	Mont Aigoual	Land	Private	X				
10	Mont Perier	Land	Private	X			X	X
11	Nîmes	Land	MF	X				
12	Pujaut	Airfield	MF	X				
13	Uzès - North	Airfield	Private		X	X		
14	Uzès – South	Land	MF	X				
15	Vic Le Fesq	Land	Private	X				

1079

1080 **Table 1. Site ID numbers and locations of the PEACH SOP1 instruments. Sites of VFRS records are**  
1081 **not indicated here. MF stands for [Météo-France](#); EMA for Ecole des Mines d'Alès.**

1082

1083

1084

1084

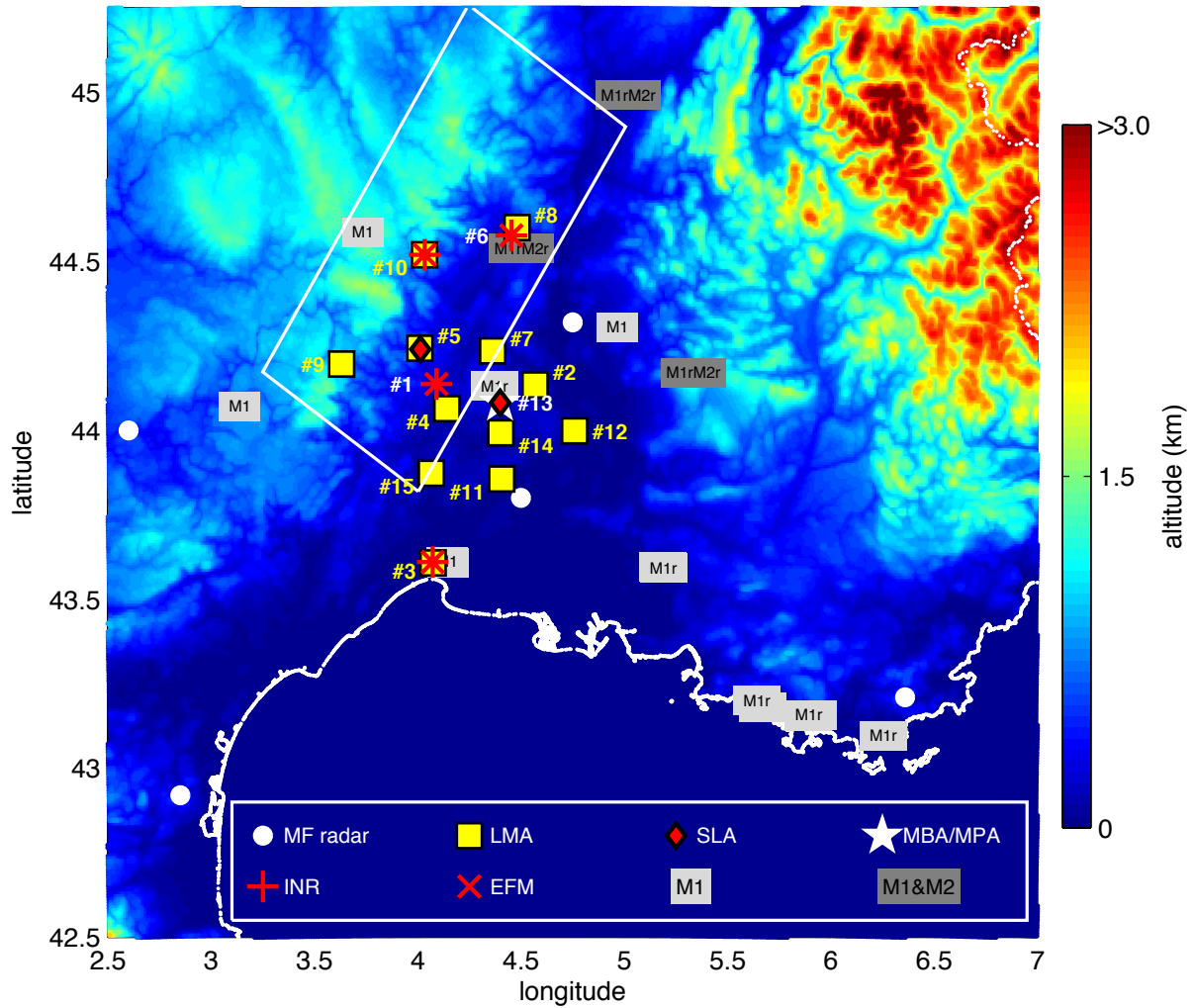
1085

Table2.eps to insert

1086

**Table 2. Status of the instruments during HyMeX SOP1 period.**

1087



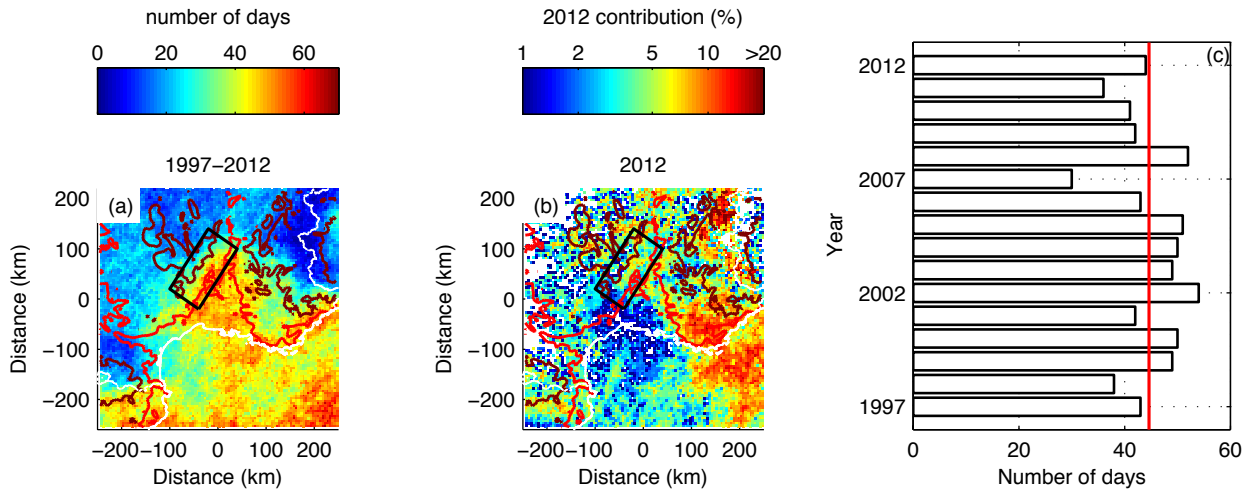
1088

1089

1090 **Figure 1 - Locations of PEACH instrumental sites (see Table 1 for details on site locations). M1**  
1091 **markers indicate VFRS locations while M2 markers indicate the few locations where**  
1092 **additionally a second video camera was operated at the same site; sites where VFRS**  
1093 **recorded actual lightning flashes are labeled with an extra letter 'r'. The Cévennes-**  
1094 **Vivarais domain is also delimited by the white polygon.**

1095

1095



1096

1097

1098

1099

1100

1101

1102

1103

1104

1105

1106

1107

1108

1109

**Figure 2 - Cloud-to-ground lightning climatology in terms of number of days with at least one cloud-to-ground lightning flash recorded per day in a regular grid of 5km x 5km and cumulated over the period investigated as sensed by Météorage from 1997 to 2012 (a), contribution of the 2012 records expressed in % relative to the 1997–2012 number of days per 5km x 5km pixel (b), and number of days per year (c) for the period September–November 2012 between over South East of France. The red solid line plotted in (c) corresponds to the average value for the 1997-2012 period. Red and dark red lines indicate 200m and 1000m height, respectively. The Cévennes-Vivarais domain is also delimited by the black polygon.**

1109

1110

F03.eps to insert

1111

1112 **Figure 3 – HyLMA records during a regular IC flash (24 September 2012, 02:02:32 UTC) with (a)**  
1113 **ground projection of the lightning records with 200m increment relief isolines, (b) latitude-altitude**  
1114 **projection of the lightning records, (c) longitude-altitude projection of the lightning records, (d)**  
1115 **250m increment histogram (bars) and cumulative distribution (red curve) of the VHF source altitude,**  
1116 **(e) time-height series of VHF sources, (f) amplitude-height series of VHF sources. The black lines**  
1117 **join the successive VHF sources recorded during the K-change event at 02:02:33.557UTC.**

1118

1119

1119  
1120  
1121  
1122  
1123  
1124  
1125  
1126  
1127  
1128  
1129  
1130  
1131  
1132  
1133

F04.eps to insert

**Figure 4 – Records during a negative CG flash with multiple ground connections (24 September 2012, 01:43:17 UTC) with (a) ground projection of the lightning records, (b) latitude-altitude projection of the lightning records, (c) longitude-altitude projection of the lightning records, (d) histogram (bars) and cumulative distribution (red curve) of the VHF source altitude, (e) time-height series of VHF sources and record of the Uzès SLA, (f) amplitude-height series of VHF sources and record of the VFRS electric field observations, (g) records of OLLSs per instrument and type of detected events available only for EUCLID and LINET. The orange bars correspond to ground strokes as identified from VFRS [Field Record](#) and video records. The VFRS location is also indicated in (a). Gray lines indicate times of all OLLS reports. Records from ATDnet, EUCLID, LINET and ZEUS are plotted with green crosses, blue symbols, red symbols, and black stars, respectively.**

1133

1134

F05.png to insert

1135

1136

**Figure 5 – Enhanced VFERS 5 ms frames recorded during the 9 ground-strokes of the -CG flash presented in Fig. 4.**

1137

1138

1138

1139

F06.eps to insert

1140

1141 **Figure 6 – Concurrent lightning records during a Bolt-from-the-blue flash recorded on 5 September**

1142

**2012 at 17:51:20UTC. See Fig. 4 for a description of each panel.**

1143

1144

1144  
1145  
1146  
1147  
1148  
1149

F07.eps to insert

**Figure 7 - LMA and OLLS records during a hybrid long-lasting flash. See Fig. 4 for a description of each panel. The relief is plotted with 500m isolines. The black isoline corresponds to 200m height.**

1149

1150

F08.eps to insert

1151

1152

**Figure 8 – Coincident observations recorded between 05:17:50 UTC and 05:20:20 UTC on 24 September 2012, with (a) ground projection of the lightning records, (b) latitude-altitude projection of the lightning records, (c) longitude-altitude projection of the lightning records, (d) 250m increment histogram (bars) and cumulative distribution (red curve) of the VHF source altitude, (e) time-height series of VHF sources and pressure difference measured at the MPA location, (f) time series of the acoustic spectrum as recorded at MPA location, and (g) records of OLLSs per instrument with in addition the time series of the Uzès SLA record.**

1154

1155

1156

1157

1158

1159

1160

1160

A F09a.eps

F09b.eps B

C F09c.eps

F09d.eps D

1161 **Figure 9 – Total lightning activity recorded at different dates with HyLMA. (a): HyMA VHF source**  
1162 **rate per 10 min period (plotted in decimal logarithmic scale); (b): ground projection of the HyLMA**  
1163 **sources during 24 h (in gray, from 00:00UTC to 23:59 UTC) and density of HyMA VHF sources**  
1164 **during one hour computed per 0.025° ×0.025° grid (in color); (c): vertical distribution of the HyLMA**  
1165 **VHF sources for the same 1 h period (and indicated at the top of the panel) per 0.025° ×200m grid.**

1166

1167

1167

E F09e.eps



F09f.eps F

1168

1169

**Figure 9 – Continued.**

1170

1171